



UNIVERSITY OF  
MARYLAND

---

## **National Transportation Center**

**Project ID: NTC2015-SU-R-02**

### **DISTRIBUTED TRAFFIC MONITORING AND PREDICTION WITH VEHICLE-TO-TO COMMUNICATION**

#### **FINAL REPORT**

by

Yingyan Lou, Ph.D.  
Arizona State University

Peiheng Li, Ph.D.  
Arizona State University

for

National Transportation Center at Maryland (NTC@Maryland)  
1124 Glenn Martin Hall  
University of Maryland  
College Park, MD 20742

**December 2017**



## **ACKNOWLEDGEMENTS**

The PI wishes to acknowledge the support from the National Transportation Center (NTC) @ Maryland for this project.

## **DISCLAIMER**

The contents of this report reflect the views of the authors, who are solely responsible for the facts and the accuracy of the material and information presented herein. This document is disseminated under the sponsorship of the U.S. Department of Transportation University Transportation Centers Program in the interest of information exchange. The U.S. Government assumes no liability for the contents or use thereof. The contents do not necessarily reflect the official views of the U.S. Government. This report does not constitute a standard, specification, or regulation.



# TABLE OF CONTENTS

<b>ACKNOWLEDGEMENTS</b> .....	<b>III</b>
<b>DISCLAIMER</b> .....	<b>III</b>
<b>TABLE OF CONTENTS</b> .....	<b>V</b>
<b>LIST OF FIGURES</b> .....	<b>VI</b>
<b>EXECUTIVE SUMMARY</b> .....	<b>1</b>
<b>1.0 INTRODUCTION</b> .....	<b>3</b>
<b>2.0 LITERATURE REVIEW</b> .....	<b>5</b>
<b>3.0 PROPOSED FRAMEWORK</b> .....	<b>7</b>
3.1 DISTRIBUTED PLATOON IDENTIFICATION.....	7
3.1.1 Micro-Discontinuity Detection .....	7
3.1.1.1 Computation Radius.....	9
3.1.1.2 Consecutive and Missing Micro-Discontinuity Flags.....	9
3.1.1.3 Threshold $\Delta$ .....	10
3.1.2 Self-Correcting Mechanism .....	11
3.2 TRAFFIC INFORMATION AGGREGATION.....	12
<b>4.0 SIMULATION RESULTS</b> .....	<b>19</b>
4.1 PLATOON DETECTION .....	19
4.2 IMPACT OF MARKET PENETRATION RATE .....	20
4.1.1 Evaluation Methodology.....	21
4.1.2 Evaluation Scenarios.....	22
4.1.3 Results Analysis.....	23
4.1.3.1 Stable Traffic.....	23
4.1.3.2 Queueing Traffic .....	28
4.1.3.3 Multi-Lane Application.....	31
4.1.3.4 Interrupted Traffic by Intersection.....	33
<b>5.0 PREDICTION ON EVOLUTION OF MICRO-DISCONTINUITY</b> .....	<b>35</b>
<b>6.0 CONCLUSIONS</b> .....	<b>40</b>
<b>7.0 REFERENCES</b> .....	<b>42</b>

## LIST OF FIGURES

Figure 1 Consecutive and Missing Micro-Discontinuity Flags .....	10
Figure 2 CDFs of Calculated Discontinuity Metric .....	11
Figure 3 Information Aggregation .....	12
Figure 4 Illustration of Calculating Vehicle Platoon Lengths .....	16
Figure 5 Platoons Detected .....	20
Figure 6 Illustration of Dynamic Road Fragmentation.....	21
Figure 7 Step-By-Step Outputs under LSHD Stable Traffic with 50% MPR .....	24
Figure 8 Step-By-Step Outputs under LSHD Stable Traffic with 90% MPR .....	25
Figure 9 Detailed Fragmentations at t=133 .....	26
Figure 10 Overall Performance Measures under Stable Traffic .....	27
Figure 11 Step-By-Step Outputs under LSHD Queueing Traffic with 90% MPR.....	29
Figure 12 Overall Performance Measures under Queueing Traffic.....	30
Figure 13 Overall Performance Measures under Stable Traffic with Two Lanes .....	32
Figure 14 Overall Performance Measures under Interrupted Traffic .....	34
Figure 15 Evolution of Platoons .....	37
Figure 16 Evolution of Micro-Discontinuity under Light Traffic .....	38
Figure 17 Evolution of Micro-Discontinuity under Heavy Traffic .....	39

## EXECUTIVE SUMMARY

This study explores an innovative framework for distributed traffic monitoring and information aggregation using vehicle-to-vehicle (V2V) communications alone. We envision the proposed framework as the foundation to an alternative or supplemental traffic operation and management system, which could be particularly helpful under abnormal traffic conditions caused by unforeseen disasters and special events. Each equipped vehicle, through the distributed protocols developed, keeps track of the average traffic density and speed within a certain range, flags itself as micro-discontinuity in traffic if appropriate, and cross-checks its flag status with its immediate up- and down-stream vehicles. The micro-discontinuity flags define vehicle groups with similar traffic states, for initiating and terminating traffic information aggregation. The framework is validated using a microscopic traffic simulation platform VISSIM and its built-in component object model. Vehicle groups are successfully identified and their average speed and density effectively estimated. The impact of market penetration rate (MPR) is also investigated with a new methodology for performance evaluation under multiple traffic scenarios. Our simulation results show that the proposed framework lends itself better to more congested traffic conditions for any given MPR. With 50% MPR, the framework is able to provide information coverage for at least 37.76% of the simulated roadway facility under various traffic scenarios. This indicates that proposed framework could be useful with an MPR as low as 50%. Even with an MRP of 20%, the coverage ratio under relatively congested traffic can still reach around 58.82%. The framework is able to provide accurate speed estimation at high spatial resolution for the simulated roadway facility. The maximum relative error is under 10% for relatively congested traffic even with MPR as low as 20%. When there is a wider range of speed distribution (less congested traffic), the worst-case maximum relative error is still under 15% when  $MPR = 20\%$ . The density estimation is more sensitive to MPR, and is more accurate under low demand and high MPR scenarios. As expected, the accuracy of both speed and density estimation increases with MPR for any given traffic scenario. It is also demonstrated that this distributed framework is able to work under queueing traffic caused by reduced speed zone, interrupted traffic introduced by intersections, and multi-lane network.





## 1.0 INTRODUCTION

With connected vehicle (CV) technologies on the horizon, we envision an alternative / supplemental traffic operation and management system for transportation networks, supported solely by vehicle-to-vehicle (V2V) designated short-range communications (DSRC). This paper investigates two of the most fundamental components of such a system—distributed traffic monitoring and platoon information aggregation. The impact of the total market penetration rate (MPR) of equipped vehicles on such a system is also examined.

The envisioned system is not meant to replace existing traffic operation practices based upon current roadway and intelligent transportation system (ITS) infrastructures, or the slew of emerging ITS's exploiting vehicle-to-infrastructure (V2I) communications, but rather as an alternative or supplemental system that is particularly suitable under abnormal traffic scenarios caused by extreme and special events. These events, such as unforeseen disasters and emergency evacuation or major sport and culture occasions, can cause unusual traffic volume and irregular spatial distribution of vehicles in transportation networks. A major disaster often paralyzes cities for an extended period, not only because of physical damages to roadway infrastructures, but also the lack of coordinated traffic control as existing traffic operation infrastructures may suffer damages as well. V2I systems or even V2V systems that rely on infrastructure (such as cellular communication technologies) may not function well either due to the same reason. V2V DSRC systems, however, would withstand this situation as long as vehicles are running in the network. On the other hand, the unusual traffic volume and patterns caused by special events may not be readily handled by existing traffic operation systems, and can add extreme stress to communication infrastructures (such as cellular base stations) due to demand surge. V2V DSRC systems, again, could prevail in this situation without causing excessive communication overhead. Therefore, we believe traffic operation and management systems based solely on V2V DSRC are a relevant concept worth investigating.

As a mobility application of connected vehicles, traffic monitoring and platoon information provision are two essential functional requirements of such a system. Constantly monitoring the traffic condition in a transportation network will enable traffic-responsive transportation operation methods that are generally more effective. With the exception of individual intersection control at a very fine detailed level, aggregate vehicular traffic pattern is often a more common and ready-to-use input to transportation operations. For example, prevailing vehicular flow rate and speed at certain locations and the evolution of vehicle queue formation in a road network is often more important than individual vehicle trajectories for arterial management and operations. On the other hand, due to communication limitations such as communication bandwidth and reliability, as well as the storage and processing capacity of (mobile and some undamaged fixed) relay and control infrastructure, not all vehicles will be able to, nor shall they do, communicate with the infrastructure individually. (This precludes machine learning or statistical classification as potential platoon identification methods as they are centralized in nature and require large amount of training data.) Therefore, the essential traffic monitoring and platoon information provision to the envisioned system must be carried out in a localized, distributed, and cooperative manner.

In this study, we have developed an innovative framework for distributed traffic monitoring and information aggregation based on V2V DSRC communications alone. Each vehicle, through the distributed protocols in the proposed framework, will keep track of the average traffic density and speed within an appropriate range (which is smaller than its communication range), and flag itself as either the lead or the anchor of a vehicle platoon (micro-discontinuity) as appropriate, utilizing fundamental concepts from traffic flow theories. To validate their own flag status, each vehicle will also engage its immediate up- and down-stream vehicles and perform a self-correction mechanism. Finally, a contention-based cooperative multi-hop protocol is developed to make sure that platoon information is aggregated in the most effective and accurate manner with minimum communication overhead. Furthermore, the impact of the market penetration rate (MPR) of equipped vehicles on the proposed framework is also investigated.

The contribution of this study is three-fold: 1) Unlike most of the relevant studies in transportation engineering, the proposed framework is a distributed traffic monitoring and aggregation approach using V2V DSRC alone. As such, the framework is not limited by the availability of roadside equipment (RSE) and can be applied to the entire transportation network. 2) Although a few distributed algorithms have been proposed in the field of vehicular ad hoc communication networks, most of them are limited to congestion detection only, and others suffer from the issue of communication overload. The proposed framework is able to monitor and report vehicular traffic information for both congested and uncongested conditions. 3) The impact of MPR is systematically examined and the proposed framework is found to deliver well even under relatively low MPR.

## 2.0 LITERATURE REVIEW

The focus of our literature review is on emerging traffic monitoring and information processing methods exploiting connected vehicle technologies. Existing research can be categorized into two groups based on whether infrastructure (both transportation and communications) is involved or not.

When supporting infrastructure is considered, V2I and other communication networks (e.g. GPS-enabled mobile phones) are the predominant underlying technologies. In this case, centralized approaches are adopted by many, if not all, previous studies. Centralized approaches rely on RSE or a server to communicate with each equipped vehicle to gather and process traffic information. For example, different methodologies have been proposed to estimate queue length at signalized intersections using probe vehicle data including travel times (Ban et al., 2011), vehicle positions (Comert and Cetin, 2011, 2009) and trajectories (Hao and Ban, 2013). Positions from probe vehicles have also been combined with signal timing plans (event-based data) to detect possible queue spillback (Christofa et al., 2013; Li et al., 2013). In He et al. (2012), a queue at an intersection is considered as a stopped platoon, and a pseudo-platoon recognition algorithm was developed based on critical headway. The estimated queue and platoon information can be used to adjust signal timings (Christofa et al., 2013; Feng et al., 2015; He et al., 2012). Goodall et al. (2013) proposed to tie individual vehicle information collected through V2I communications within an intersection into a real-time simulation-in-the-loop traffic signal timing optimization program. It can be seen from the aforementioned studies that, due to the requirement of RSE or the limited bandwidth of other communication networks (e.g., cellular network), mobility applications of the centralized approaches are limited to intersections, or otherwise relatively small areas.

Vehicular ad hoc network, on the other hand, does not require RSE or other communication infrastructures. It is intensively based on V2V communications and distributed computing. One of its major applications is traffic condition monitoring and information dissemination (e.g. Fukumoto et al, 2007). However, each individual vehicle periodically transmitting its local vehicular traffic information in addition to broadcasting general beacons may result in additional communication load. To relief the potential communication overload, a “need to say” principle is usually adopted (Dornbush and Joshi, 2007). Therefore, information aggregation and dissemination is restricted to extreme conditions such as traffic congestion or incidents (Bauza et al., 2010; Lakas and Cheqfah, 2009; Lin and Osafune, 2011; Terroso-sáenz et al., 2012; Vaqar and Basir, 2009). These works often adopt data aggregation as an additional approach to reducing communication load. Generally, each vehicle would periodically estimate its local congestion level from received beacons. The congestion level is usually measured by density (Fukumoto et al., 2007; Terroso-sáenz et al., 2012), speed (Lin and Osafune, 2011), or travel time (Lakas and Cheqfah, 2009), etc. Bauza et al. (2010) adopted a fuzzy logic to determine local congestion level using both density and speed. Each vehicle then compares its local congestion level with a predefined threshold to determine whether to trigger information aggregation or not. Once triggered, a cooperative protocol will assemble and pass on aggregate information about the congestion encountered, including its position, size and congestion level, instead of the local

traffic condition from each individual vehicle (e.g. Bauza et al., 2010). One limit of the “need to say” principle is that no information is available for uncongested sections of the road. However, both uncongested (especially near capacity) and congested traffic states are valuable to mobility applications for large and complex transportation networks. Huang et al. (2010) also proposed a distributed congestion detection and prediction algorithm. Unlike other studies, it employs the concept of shockwave and is only applicable to merging bottlenecks. Furthermore, all of the above studies assumed 100% MPR. At the early stage of CV implementations, a relatively low MPR is expected and it is important that any proposed distributed algorithms would work relatively well under such a condition.

The new framework proposed in this study has many benefits from previous research without suffering from some of the drawbacks. A platoon identification approach takes advantage of traffic flow theory. Aggregated traffic information under both uncongested and congested conditions is monitored and reported for the entire road network. A contention-based forwarding protocol reduces the communication overhead. The proposed framework also performs relatively well even under low MPRs.

## 3.0 PROPOSED FRAMEWORK

The proposed framework consists of two major components: 1) distributed traffic monitoring for platoon identification and 2) cooperative platoon information aggregation. The former involves two processes: micro-discontinuity detection and self-correction; and the latter three: initiation, re-transmission, and termination.

### 3.1 DISTRIBUTED PLATOON IDENTIFICATION

A platoon is a group of vehicles with similar states. This simple statement is in fact ambiguous: the terms “similar” and “state” are both subject to interpretation. To identify a platoon, the metric(s) to determine “state” and the threshold(s) to define “similar” must be specified. Space and time headway measures such as critical and cumulative headways are often adopted as metrics for platoon recognition both in the literature (Chaudhary et al., 2003; He et al., 2012; Jiang et al., 2006) and in practice. Most of such approaches require infrastructure, and are not able to effectively pinpoint vehicular traffic state variation. As Huang et al. (2010) pointed out, individual headways may fluctuate substantially even among a group of vehicles with the same speed. In this case, using headway as the metric would likely result in significantly more platoons being reported than necessary. Therefore, except for intersection signal timing, headways are not suitable as the metric for platoon identification.

Alternatively, if we consider a platoon as a group of vehicles with similar states, then two adjacent platoons should display different traffic states, in terms of both platoon density and speed. The boundary vehicles of the two platoons should be able to detect such difference, which we term micro-discontinuity to differentiate it from the concept of shockwave (Lighthill and Whitham, 1955; Richards, 1956; Stephanopoulos et al., 1979) in macroscopic traffic flow theory. Thus, platoon identification becomes micro-discontinuity identification, and the problem now lends itself very well to distributed computing based on V2V DSRC.

#### 3.1.1 Micro-Discontinuity Detection

In first-order continuum traffic flow models (Jin and Yang, 2013; Lighthill and Whitham, 1955; Richards, 1956), the vehicular traffic state at location  $x$  and time point  $t$ , denoted by  $s(x, t)$ , is defined by two field functions: density  $k(x, t)$  and speed  $v(x, t)$ . The models are macroscopic in nature, and describe traffic dynamics with a partial differential equation. Shockwaves represent abrupt changes in the traffic state over continuous space and time, and are in fact mathematical discontinuities in these macroscopic models.

Due to limited communication range, the proposed distributed traffic state monitoring is conducted at a microscopic level. Therefore, direct application of the concept of shockwave from continuum traffic flow models is inappropriate, and a new methodology is needed to quantitatively define micro-discontinuity.

For an equipped vehicle  $i$ , denote its down- and up-stream traffic states at the  $n^{\text{th}}$  time interval as  $s(x_i^d, n\Delta t)$  and  $s(x_i^u, n\Delta t)$ , where  $x_i^d$  and  $x_i^u$  represent the lengths of road fragments in

consideration down- and up-stream. The choice of  $x_i^d$  and  $x_i^u$  will be discussed later, but they must be within the communication range of vehicle  $i$ .

$$s(x_i^d, n\Delta t) := \begin{cases} k(x_i^d, n\Delta t) = \frac{|N_i^d(n\Delta t)|}{x_i^d} \\ v(x_i^d, n\Delta t) = \frac{1}{|N_i^d(n\Delta t)|} \sum_{j \in N_i^d(n\Delta t)} v_j(n\Delta t) \end{cases}$$

where  $N_i^d(n\Delta t)$  is the subset of vehicles which are in  $x_i^d$  at time  $n\Delta t$ , and  $|\cdot|$  denotes cardinality.  $v(x_i^d, n\Delta t)$  is in fact the space-mean speed. Note that  $s(x_i^u, n\Delta t)$  is defined similarly, and vehicle  $i$  itself is not included in  $s(x_i^d, n\Delta t)$  or  $s(x_i^u, n\Delta t)$ . We further define the following variables:

$$\begin{aligned} \Delta_v(i, n\Delta t) &:= v(x_i^u, n\Delta t) - v(x_i^d, n\Delta t) \\ \Delta_k(i, n\Delta t) &:= k(x_i^u, n\Delta t) - k(x_i^d, n\Delta t) \end{aligned}$$

The metric for micro-discontinuity detection is subsequently defined as  $\Delta_s(i, n\Delta t) := |\Delta_v(i, n\Delta t)| + |\Delta_k(i, n\Delta t)|$ , which is the 1-norm of vector  $(\Delta_v(i, n\Delta t), \Delta_k(i, n\Delta t))$ . Vehicle  $i$  is said to have detected a micro-discontinuity if  $\Delta_s(i, n\Delta t)$  is greater than a predefined threshold value  $\Delta$  (to be discussed later). It will then set a flag  $f(i, n\Delta t)$  in its own memory for future computation. Common cases of micro-discontinuity can be observed when a queue is being formed or discharged, in a moving bottleneck, and a group of loosely spaced vehicles traveling at similar speeds etc.

Since a platoon is uniquely defined by a lead and an anchor vehicle, we further differentiate a lead micro-discontinuity flag from an anchor flag, and an isolated vehicle is considered a special micro-discontinuity. The following pseudocode describes the identification process.

**process** *micro-discontinuity identification* // each vehicle  $i$  performs this process at time  $n\Delta t$

**begin**

set  $f(i, n\Delta t) = 0$ ;

calculate  $\Delta_s(i, t)$ ;

**if**  $(\Delta_s(i, t) \geq \Delta$  and  $\Delta_k(i, t) > 0)$  or  $(|N_i^d(t)| = 0$  and  $|N_i^u(t)| > 0)$  **then**

$f(i, t) = 1$ ; // lead vehicle

**if**  $(\Delta_s(i, t) \geq \Delta$  and  $\Delta_k(i, t) < 0)$  or  $(|N_i^u(t)| = 0$  and  $|N_i^d(t)| > 0)$  **then**

$f(i, t) = -1$ ; // anchor vehicle

**if**  $|N_i^d(t)| = |N_i^u(t)| = 0$  **then**

$f(i, t) = 2$ ; // isolated vehicle

**end;**

In the above pseudocode, the values of  $x_i^d$ ,  $x_i^u$  and  $\Delta$  need additional specification. The determination of  $\Delta$  is further related to consecutive and missing micro-discontinuity flags of the same type.

### **3.1.1.1 Computation Radius**

Although  $x_i^d$  and  $x_i^u$  can take any value, it is essential to a distributed algorithm that these values stay constant across individual vehicles. Denote  $r_c = x_i^d = x_i^u$  as the computation radius for traffic state determination. Obviously, the communication range of CV's,  $r$  (usually from 200 to 300 meters for DSRC), is the upper bound of  $r_c$ . Existing research on congestion detection based on vehicular ad hoc networks does not differentiate  $r_c$  from  $r$ , and usually set  $r_c = r$  (Bauza et al., 2010; Fukumoto et al., 2007). However, the communication range is often too large for the distributed algorithm to detect sizable headways within the range. For example, suppose all vehicles are traveling at constant speed  $v$ , and there is a sizeable headway between vehicles  $j$  and  $k$ . From a traffic operations perspective (for example, traffic signal timing), it is possible that these vehicles should be treated as two platoons. But with  $r_c = r$ , vehicles  $k$  and  $j$  may not detect any difference between their downstream and upstream traffic conditions, and would consider themselves as part of a single platoon. To avoid this problem,  $r_c$  is set to 50 meters in this study. This is not to say that the minimum space headway the algorithm is able to detect is 50 meters. We will further demonstrate this in Section 4 Simulation Results.

### **3.1.1.2 Consecutive and Missing Micro-Discontinuity Flags**

It is possible that multiple consecutive vehicles within close vicinity will flag the same type of micro-discontinuity. An example of a queue being formed is shown in Figure 1 where the first three stopped vehicles all flag lead micro-discontinuity. With  $r_c = 50\text{m}$  and no vehicle further downstream, vehicles 1 – 3 could all detect a much more congested traffic state upstream, and flag themselves as the lead.

On the other hand, it is also possible that vehicles at the boundaries of potential platoons may not flag themselves as micro-discontinuities. As shown in Figure 1, vehicle  $k$  is supposed to be the lead of the vehicle platoon consisting of vehicles  $k$  to  $l$ , but it did not flag itself as a discontinuity since its downstream and upstream traffic states are very similar.

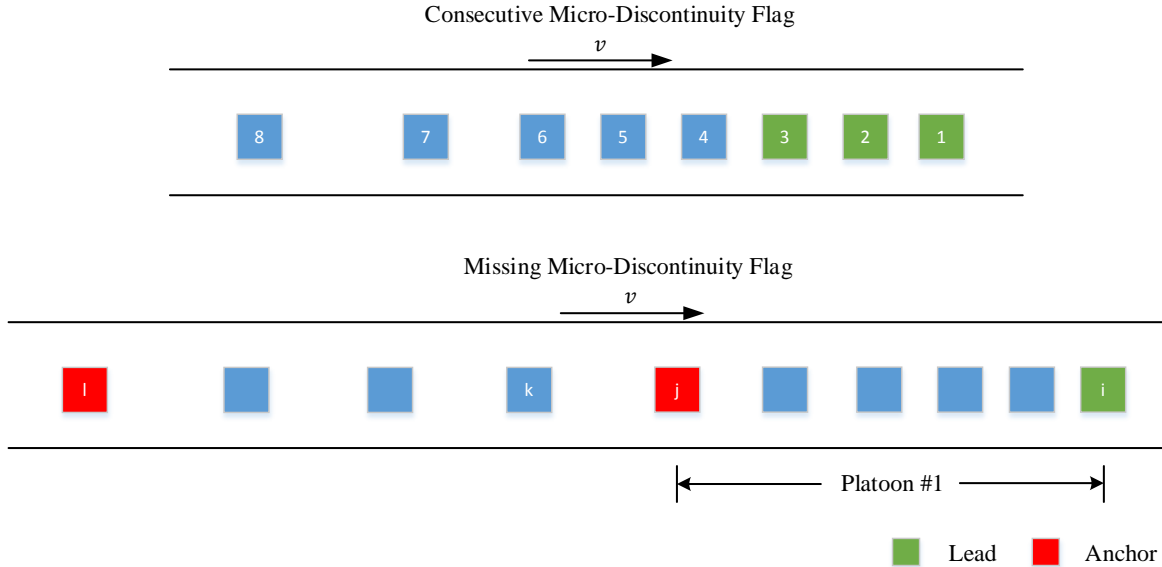


**Figure 1 Consecutive and Missing Micro-Discontinuity Flags**

Such consecutive and missing discontinuity flags cause problems in the determination of vehicle groups, and should be resolved and avoided if possible. To reduce the number of consecutive flags generated, the value of the threshold  $\Delta$  should be chosen carefully. Furthermore, to clean up consecutive and correct missing flags when they do occur, a self-correcting mechanism is proposed.

### 3.1.1.3 *Threshold $\Delta$*

A good threshold should allow us to correctly identify potential micro-discontinuities while minimizing the number of consecutive discontinuities. The value of  $\Delta$  is related to the computation radius  $r_c$ . We performed a series of tests using microscopic traffic simulation to find a good threshold value with  $r_c = 50\text{m}$ . A straight single-lane road segment was built in VISSIM 6 for this purpose. Different free-flow speeds (FFS's) from 40 km/h to 120 km/h were tested. Figure 2 shows the cumulative density function (CDF) of  $\Delta_s$  computed by all simulated vehicles over a 200-second simulation. It can be seen that regardless of the FFS, the increase of the CDFs becomes gradual and smooth when  $\Delta_s \geq 75$ , which is approximately the 70<sup>th</sup>-percentile value. In other words, if  $\Delta = 75$ , about 30% of vehicles will flag themselves as micro-discontinuities. A manual check confirmed that when  $\Delta = 75$ , the issue of consecutive micro-discontinuity flags of the same type is not pronounced. It is also possible to adopt any value higher than 75 as a potential threshold. However, a rather high threshold value may lead to a very low identification rate of potential micro-discontinuities (and thus platoons). In this sense,  $\Delta = 75$  is a reasonable threshold. Note that we do not intend to find an “optimal”  $\Delta$  in this study, as there is arguably a well-defined optimality condition.



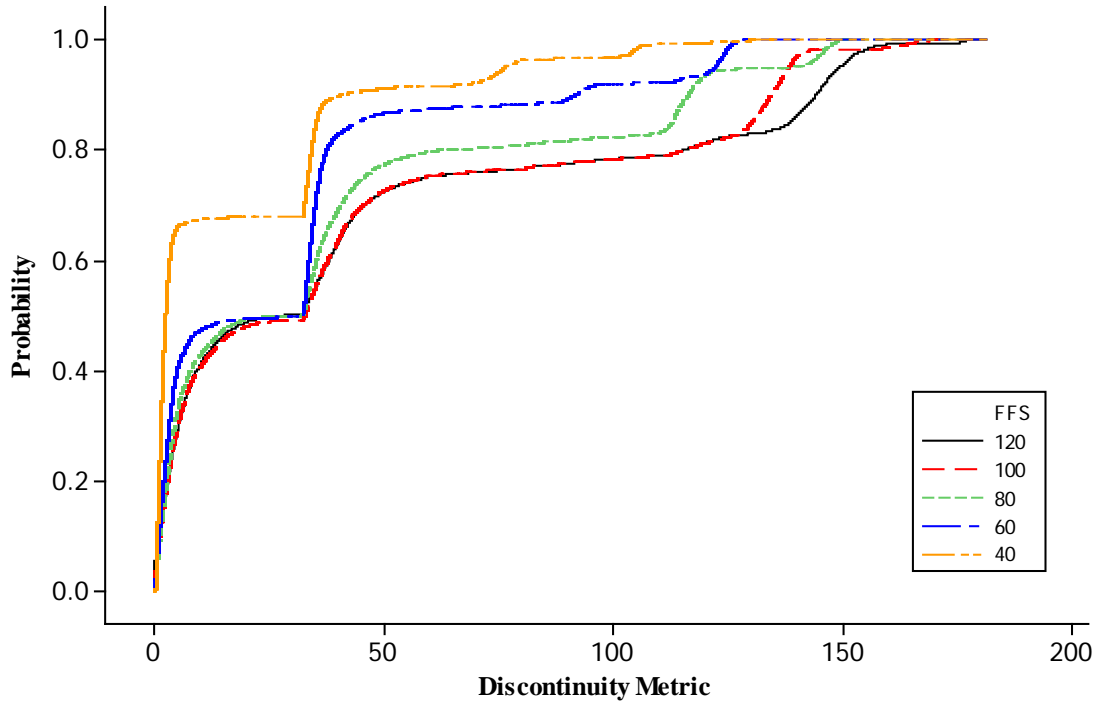


Figure 2 CDFs of Calculated Discontinuity Metric

### 3.1.2 Self-Correcting Mechanism

Even with a carefully-chosen threshold value, consecutive and missing micro-discontinuity flags may still occur due to intrinsic randomness in traffic. To resolve these problems, a self-correcting mechanism is proposed.

The micro-discontinuity identification process is performed every time interval. In this study, the interval  $\Delta t$  is set to one second. A small time lag  $\varepsilon$ ,  $\varepsilon \ll \Delta t$ , after the process is finished, each vehicle will launch the self-correcting mechanism to check the status of its immediate downstream (if itself is a lead) or upstream (if itself is an anchor) vehicle, if there is any vehicle within its computation range. If the other vehicle has 1) no flag, the vehicle will send a message to the other vehicle to correct the missing flag; 2) same type of flag, the vehicle simply removes its own flag; 3) a different type of flag, the vehicle does nothing. This is equivalent to setting the first (last) vehicle with a lead (an anchor) flag the actual lead (anchor) of the platoon. The following pseudo code details the self-correcting mechanism. For convenience, assume vehicles are numbered ascendingly from downstream to upstream.

```

process self-correcting mechanism //every vehicle  $i$  performs this process at time  $n\Delta t + \varepsilon$ 
begin
    if  $f(i, n\Delta t) \neq 0$  then

```

```

if  $f(i, n\Delta t) = 1$  and  $|N_i^d(n\Delta t)| > 0$  then
    //check the flag status of its immediate downstream vehicle  $f(i - 1, n\Delta t)$ 
    if  $f(i - 1, n\Delta t) = 0$  then // no anchor
        send message  $Anchor(i - 1, n\Delta t)$  to vehicle  $i - 1$  and set
         $f(i - 1, n\Delta t) = -1$ ;
    if  $f(i - 1, n\Delta t) = 1$  then // consecutive leads
        set  $f(i, n\Delta t) = 0$ ;
    if  $f(i, n\Delta t) = -1$  and  $|N_i^u(n\Delta t)| > 0$  then
        //check the flag status of its immediate upstream vehicle
         $f(i + 1, n\Delta t)$ 
        if  $f(i + 1, n\Delta t) = 0$  then // no lead
            send message  $Lead(i + 1, n\Delta t)$  to vehicle  $i + 1$  and set
             $f(i + 1, n\Delta t) = 1$ ;
        if  $f(i + 1, n\Delta t) = -1$  then // consecutive anchors
            set  $f(i, n\Delta t) = 0$ ;
end;

```

### 3.2 TRAFFIC INFORMATION AGGREGATION

Once platoons are identified, a contention-based cooperative multi-hop protocol is developed to make sure that platoon information is aggregated in the most effective and accurate manner with minimum communication overhead. The identified lead vehicles will start a cooperative traffic information aggregation protocol, a process of forwarding and aggregating local traffic information through multi-hop V2V DSRC. This process could be initiated at time  $n\Delta t + 2\varepsilon$ . Figure 3 provides an illustration of the concept.

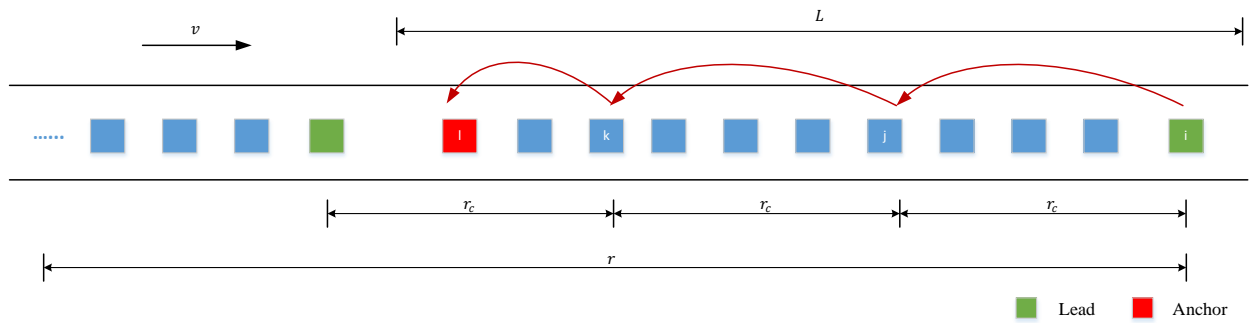


**Figure 3 Information Aggregation**

The local information forwarding during an aggregation process will follow “the most forwarded within-range” manner (Jin and Recker, 2006). As shown in Figure 3, the local information computed by the lead vehicle  $i$  will be forwarded to the furthest upstream vehicle  $j$  within its

computation range  $r_c$ , processed by vehicle  $j$  to incorporate the local information computed by vehicle  $j$ , forwarded again in a similar manner, and finally terminated at the anchor vehicle  $l$  of the group.

In order to achieve this, a modified contention-based forwarding protocol is proposed based on methods described in Füßler et al. (2003) and Bauza et al. (2010). A lead vehicle  $i$  will first broadcast the initial aggregation request  $aggInfo(i, i, n\Delta t)$  with its local traffic information. In this notation, the first argument denotes that the message is sent by vehicle  $i$ ; later this argument will be updated according to the relaying vehicle  $j$  of this message. The second and third arguments indicate that the aggregation request is originally initiated by lead vehicle  $i$  for traffic information at time  $t = n\Delta t$ . A pseudocode is provided below detailing the content of  $aggInfo(j, i, n\Delta t)$ .

**message**  $aggInfo(j, i, n\Delta t)$

**begin**

**version:** version number to document updates in the aggregation process, equals to 1 when first broadcasted by a lead vehicle  $i$ ;

**time stamp:** time of last update of  $aggInfo(i, n\Delta t)$ , equals to  $n\Delta t$  when first broadcasted by a lead vehicle  $i$ ;

**lead vehicle info:** lead vehicle ID ( $i$ ) and position;

**sending vehicle info:** sending vehicle ID ( $j$ ) and position;

**local traffic info:** length, aggregated density and speed of the vehicle platoon led by vehicle  $i$ ;

**end;**

In fact, when a lead vehicle  $i$  sends  $aggInfo(i, i, n\Delta t)$ , every vehicle within its communication range  $r$  (both down- and up-stream) will receive the message. Downstream vehicles, as well as upstream vehicles beyond  $r_c$  should simply discard the cooperative aggregation request. The latter is because the local traffic information from vehicle  $i$  is valid only for the computation range  $r_c$ . Among the upstream vehicles, only vehicle  $j$ , the furthest within vehicle  $i$ 's computation range needs to process and relay the information. It is possible for vehicle  $j$  to receive multiple aggregation requests simultaneously from downstream, and these requests will be stored in a re-transmission queue. If this is the case, only the request from the closest lead / relaying vehicle is considered to be active and all other requests will be discarded. If the anchor vehicle  $l$  of the platoon led by  $i$  is within  $r_c$  from vehicle  $i$  but not the furthest in this range, the anchor vehicle should broadcast a termination message  $terminate(l, i, n\Delta t)$  right away with a reasonably small time lag. Once other vehicles receive this termination message, they will discard  $aggInfo(i, i, n\Delta t)$  before it is time for any of them to relay the information. To achieve this, each upstream vehicle  $j$  within  $r_c$  of vehicle  $i$  will set a distance-based timer for re-transmitting  $aggInfo(i, i, n\Delta t)$  or terminating the process:

$$timer(i, j, n\Delta t) = \begin{cases} \frac{1}{distance(i, j, n\Delta t)} & \text{if } f(j, t) = 0 \\ \frac{1}{distance(i, j, n\Delta t) + r_c} & \text{if } f(j, t) = -1 \end{cases}$$

The pseudocodes below describe the initiation, re-transmission, and termination processes of the cooperative information aggregation protocol respectively. The re-transmission process also involves a sub-process that updates the aggregated traffic information. Details of this sub-process is further discussed at the end of this section.

**process** *initiate aggregation* // each lead vehicle  $i$  performs this process at time  $n\Delta t + 2\varepsilon$

**begin**

**if**  $f(i, n\Delta t) = 1$  **then**

generate message  $aggInfo(i, i, n\Delta t)$ ;

broadcast cooperative aggregation request  $aggInfo(i, i, n\Delta t)$ ;

**end;**

**process** *re-transmit* // each vehicle  $k$  performs this process upon receiving  $aggInfo(j, i, n\Delta t)$  at time  $t$

**begin**

**if**  $t \in (n\Delta t + 2\varepsilon, n\Delta t + \Delta t)$  and  $k \in N_j^u(n\Delta t)$  **then**

set Boolean  $isupdate(j, i, n\Delta t) = \text{false}$ ;

**if** the re-transmission queue of vehicle  $j$  is empty **then**

$isupdate(j, i, n\Delta t) = \text{true}$ ;

**else**

// if multiple  $aggInfo$  messages from different downstream lead vehicles are received by vehicle  $k$

**if** vehicle  $i$  is closer to  $k$  than any other lead vehicle  $p$  with  $aggInfo(q, p, n\Delta t)$  in the re-transmission queue of vehicle  $k$  **then**

$isupdate(j, i, n\Delta t) = \text{true}$ ;

discard  $aggInfo(q, p, n\Delta t)$ ,  $\forall p$  further downstream of  $i$ ;

// if multiple  $aggInfo$  messages from the same downstream lead vehicle but different downstream relay vehicles are received by vehicle  $k$

**if** vehicle  $j$  is closer to  $k$  than any other relay vehicle  $q$  with  $aggInfo(q, i, n\Delta t)$  in the re-transmission queue of vehicle  $k$  **then**

$isupdate(j, i, n\Delta t) = \text{true}$ ;

discard  $aggInfo(q, i, n\Delta t)$ ,  $\forall q$  further downstream of  $j$ ;

// vehicle  $k$  is the next relay vehicle and the message  $aggInfo(j, i, n\Delta t)$  will be updated up to vehicle  $k$

**if**  $isupdate(j, i, n\Delta t) == \text{true}$  **then**

    call **process**  $aggInfoUpdate$  to revise **message**  $aggInfo(j, i, n\Delta t)$  to **message**  $aggInfo(k, i, n\Delta t)$ ;

**if**  $f(k, n\Delta t) = 0$  **then**

        set  $timer(j, k, n\Delta t) = \frac{1}{distance(j, k, n\Delta t)}$ ;

        store **message**  $aggInfo(k, i, n\Delta t)$  in the re-transmission queue of vehicle  $k$  for broadcasting at  $t + timer(j, k, n\Delta t)$ ;

**if**  $f(k, n\Delta t) = -1$  **then**

        set  $timer(j, k, n\Delta t) = \frac{1}{distance(j, k, n\Delta t) + r_c}$ ;

        store **message**  $termInfo(k, i, n\Delta t)$  in the re-transmission queue of vehicle  $k$  for broadcasting at  $t + timer(j, k, n\Delta t)$ ;

**else** discard  $aggInfo(j, i, n\Delta t)$ ;

**else** discard  $aggInfo(j, i, n\Delta t)$ ;

**end;**

**process**  $terminate$  // each vehicle  $k$  performs this process upon receiving  $termInfo(l, i, n\Delta t)$  at time  $t$

**begin**

**if**  $t \in (n\Delta t + 2\varepsilon, n\Delta t + \Delta t)$  **then**

        discard  $aggInfo(j, i, n\Delta t)$ ,  $\forall j$  in the re-transmission queue of vehicle  $k$ ;

**else** discard  $termInfo(l, i, n\Delta t)$ ;

**end;**

When updating the message  $aggInfo(j, i, n\Delta t)$  to  $aggInfo(k, i, n\Delta t)$ , vehicle  $k$  would first check the version number of  $aggInfo(j, i, n\Delta t)$ . Denote this version number as  $m$ , which is in fact the number of hops performed so far. Denote the length of the vehicle platoon up to the  $m^{th}$  ( $m \geq 1$ ) update as  $L_m$ . For the  $(m + 1)^{th}$  update being performed by vehicle  $k$ ,

$$L_{m+1} = L_m + distance(j, k, n\Delta t)$$

where  $j$  is the previous, and  $k$  the current, sending vehicle of the message. Note  $L_1$  (i.e.  $m = 1$ ) is the distance between the lead vehicle and the front virtual boundary of the platoon (see Figure 4). If vehicle  $k$  is the anchor vehicle of the platoon led by vehicle  $i$ , then the  $(m + 1)^{th}$  update is also the last update, and

$$L_{m+1} = L_m + \text{distance}(j, k, n\Delta t) + L_{-1}$$

where  $L_{-1}$  is the distance between the anchor vehicle and its rear virtual boundary. The determination of  $L_1$  and  $L_{-1}$  is not trivial. In the case as shown in Figure 4, if the distance between an anchor vehicle  $j$  and a lead vehicle  $k$  is less than  $2r_c$ , the virtual boundary (the actual separation) of the two adjacent platoons is defined as the middle point between the two boundary vehicles. In this case,  $L_1$  for the second platoon is the same as  $L_{-1}$  of the first platoon, equal to half the distance between vehicle  $k$  and vehicle  $j$ . The final lengths of the two platoons are  $L$  and  $L'$  as seen in Figure 4.

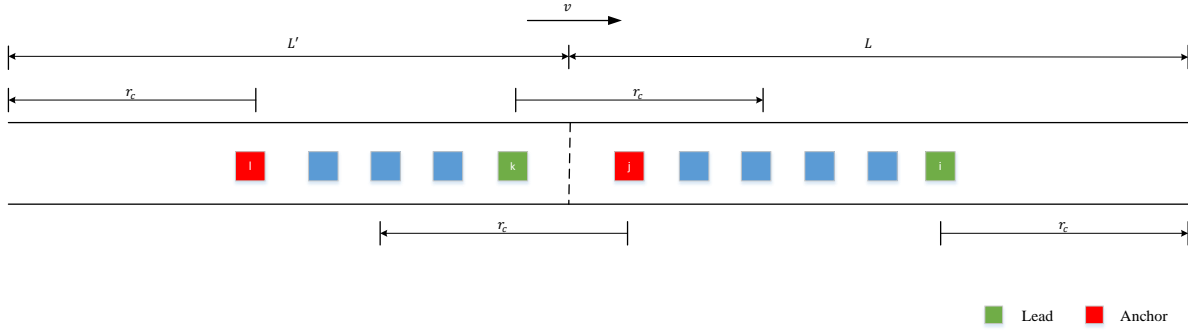


**Figure 4 Illustration of Calculating Vehicle Platoon Lengths**

The total number of vehicles in the group is updated as

$$Num_{m+1} = Num_m + Num(j, k, n\Delta t)$$

where  $Num(j, k, n\Delta t)$  is the number of vehicles between vehicles  $j$  (excluding  $j$ ) and  $k$  (including  $k$ ) at time  $n\Delta t$ , and  $Num_1 = 1$ .

The group density after the  $(m + 1)^{th}$  hop is calculated as

$$GD_{m+1} = \frac{Num_{m+1}}{L_{m+1}}$$

For an isolated vehicle, there is only itself in the group and the group density is defined as

$$GD_1 = \frac{1}{L_{-1} + L_1}$$

Similarly, the average speed of the platoon is updated as follows:

$$GS_{m+1} = \frac{Num_m \cdot GS_m + \sum_{p=j+1}^k v_p(n\Delta t)}{Num_{m+1}}$$

The initial average speed is essentially the speed of the lead/isolated vehicle  $i$  at time  $t = n \Delta t$ , i.e.  $GS_1 = v_i(n\Delta t)$ .

The following pseudocode shows the process of updating aggregation information, which is a sub-routine of the information forwarding process (process *re-transmit*).

**process** *aggInfoUpdate*// performed by relaying and / or terminating vehicles *k* as a sub-process of **process** *re-transmit*

**begin**

$m = m + 1;$

**If**  $f(j, n\Delta t) = 0$  **then**

$L_m = L_{m-1} + \text{distance}(j, k, n\Delta t);$

**If**  $f(j, n\Delta t) = -1$  **then**

$L_m = L_{m-1} + \text{distance}(j, k, n\Delta t) + L_{-1};$

$Num_m = Num_{m-1} + Num(j, k, n\Delta t);$

$GD_m = \frac{Num_m}{L_m};$

$GS_m = \frac{Num_{m-1} \cdot GS_{m-1} + \sum_{p=j+1}^k v_p(n\Delta t)}{Num_m};$

**end;**

Upon termination of the information aggregation protocol, the group density, average speed, number of vehicles, and length will be available immediately. The aggregated information can be disseminated to all vehicles on the network and signal controllers through multi-hop V2V communications. Such information dissemination is beyond the scope of this study and will be explored in our future research.





## 4.0 SIMULATION RESULTS

The proposed framework is implemented in Visual Basic with a microscopic traffic simulation package VISSIM and its built-in component object model (COM). Two types of traffic conditions, stable traffic and queueing, are simulated and analyzed in this study. A one-lane segment is used for our experiments. We further analyzed the impacts of MPR on the performance of our proposed framework under both stable and queueing traffic.

### 4.1 PLATOON DETECTION

For stable traffic, the single-lane road segment is simulated as a freeway section without any merges or diverges. The proposed distributed framework is able to identify vehicle platoons in a reasonable manner. Stable traffic in Figure 5 shows snapshots of the road segment in 5 consecutive seconds. Blue rectangles represent vehicles that did not flag traffic discontinuity. Green and red rectangles are vehicles self-identified as leads and anchors, respectively. In this stable-traffic experiment, no consecutive flags of the same type are reported. As shown in the top subfigure in Figure 5, there are two vehicle platoons at  $t = 0, 1, 4$  second. At  $t = 2$  and 3 second, the fourth vehicle from downstream reported itself as an isolated vehicle (shown in black) since there was no vehicle within its computation range both up- and down-stream. Note that at  $t = 4$  second, this vehicle became the anchor of the first vehicle platoon as it got closer to the first three vehicles. One noteworthy observation is that in stable traffic, the speeds of different vehicles are similar, and vehicle positions/headways (and thus densities) largely affect identified platoons.

Queueing scenarios present more complicated traffic conditions where multiple consecutive flags of the same type may occur. The proposed framework is able to resolve this issue with the self-correcting mechanism and identify reasonable vehicle platoons. The bottom two subfigures in Figure 5 are results from an experiment with a traffic signal at the immediate downstream of the simulated segment. They are snapshots of 11 consecutive seconds during which the signal was red and a queue was being formed. For the first two seconds ( $t = 65, 66$ ), only one vehicle group is reported with a single lead and a single anchor. Starting from  $t = 67$  second, multiple consecutive discontinuity flags of the same type were reported (see Before Self-Correction in Figure 5). As the first several vehicles pulled into full stop, they all identified themselves as leads. This is because the average upstream density within their computation range is higher comparing to the downstream traffic, and so is speed as there was no vehicle further downstream of the signal. At  $t = 71$  second, vehicle 6 flagged itself as an anchor. In the next 5 seconds, multiple consecutive anchor flags were reported by vehicles 6 – 9 as they joined the queue. Two problems were raised in this particular scenario: 1) multiple consecutive discontinuity flags of the same type, and 2) no vehicle flagged itself as an anchor (lead) immediately downstream (upstream) of the group of multiple lead (anchor) flags. These problems, however, are successfully addressed by the self-correction mechanism as part of the proposed framework (see After Self-Correction of Figure 5).



**Figure 5 Platoons Detected**

As described in Section 3.1, the self-correcting mechanism simply identifies the first (furthest downstream) lead vehicle as the actual start of a vehicle platoon (vehicle 1 in this example, see After Self-Correction in Figure 5), and the last (furthest upstream) anchor vehicle as the actual end of a vehicle platoon (vehicle 7 at  $t = 72$ , vehicle 8 at  $t = 73, 74$ , and vehicle 9 at  $t = 75$ ). According to the mechanism, these vehicles would also send a request to their immediate downstream (upstream) neighbors to flag the opposite type of discontinuity. In this example, vehicle 7 at  $t = 71$ , vehicle 8 at  $t = 72$ , vehicle 9 at  $t = 73, 74$ , and vehicle 10 at  $t = 75$  were marked as lead per request from the vehicle they were following.

## 4.2 IMPACT OF MARKET PENETRATION RATE

Since our proposed framework for traffic condition monitoring is distributed and relies on equipped vehicles, a low MPR may affect its effectiveness and accuracy. Note that vehicle platoons essentially divide a road segment into a set of fragments in a dynamic manner. With 100% MPR, traffic information is available for every fragment. Even when there is radio silence between two platoons, it is straightforward to conclude that there is no vehicle present in the fragment defined by the gap between these two platoons. In this sense, the proposed framework is able to achieve 100% coverage of a road segment with 100% MPR. On the other hand, a lower MPR will not only lead to a lower coverage ratio, the aggregated information may also be inaccurate due to the presence of non-equipped vehicles in a platoon.

To quantitatively analyze the impact of MPR, we consider the aggregated traffic condition under 100% MPR as the ground truth, and compare results from lower MPR scenarios to the ground

truth in terms of both coverage ratio and relative errors of aggregated density and speed. The former evaluates the effectiveness, and the latter the accuracy, of the proposed distributed traffic monitoring framework.

Our results indicate that the average coverage ratio increases with MPR. A decreasing relationship is also observed between the average relative error in density/speed and MPR. Free flow speed and traffic demand level both affect the performance of the proposed framework.

#### 4.1.1 Evaluation Methodology

For convenience, denote 100% MPR as case  $g$  and a  $p\%$  MPR as case  $p$ , where  $0 < p < 100$ . To compare cases  $p$  and  $g$  on a fair ground, we first combine their fragmentation (platooning) as illustrated in Figure 6. Note that the figure only shows the fragmentation at a specific time interval, and the fragmentation will evolve with time as the traffic dynamics evolve.

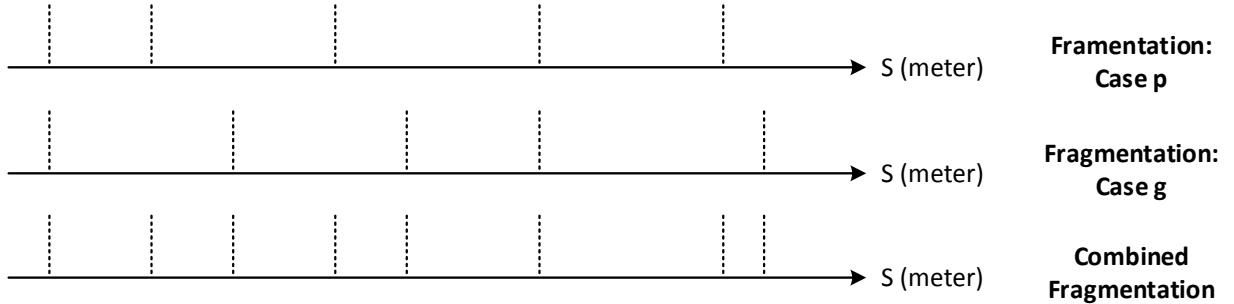


**Figure 6 Illustration of Dynamic Road Fragmentation**

This allows us to compare the differences in traffic states for each fragment between cases  $p$  and  $g$ . The sum of the relative differences of each fragment, weighted by fragment length, over the entire road segment is considered another overall performance measure.

Denote the traffic state of fragment  $x$  at time  $t$  under case  $g$  as  $s_g(x, t) = (k_g(x, t), v_g(x, t))$  and that under case  $p$  as  $s_p(x, t) = (k_p(x, t), v_p(x, t))$ . If fragment  $x$  is not covered by equipped vehicles under case  $p$ , then  $s_p(x, t) = \Phi$  (no information available), and this fragment is excluded from the accuracy evaluation. Let  $L_g$  and  $L_p$  represent the total lengths of the covered segments under cases  $g$  and  $p$ . Note that  $0 < L_p(t) \leq L_g(t) = L$ . The coverage ratio can then be mathematically defined as

$$cr_p(t) = \frac{L_p(t)}{L_g(t)}$$

When  $s_p(x, t) \neq \Phi$ , define the relative error in density of segment  $x$  at time  $t$  as

$$re_{density}(x, t) = \frac{|k_p(x, t) - k_g(x, t)|}{k_g(x, t)}$$

Similarly, the relative error in speed is defined as

$$re_{speed}(x, t) = \begin{cases} \frac{|v_p(x, t) - v_g(x, t)|}{v_g(x, t)} & \text{if } v_g(x, t) > 0 \\ 0 & \text{if } v_g(x, t) = 0 \end{cases}$$

Note that  $k_g(x, t)$  is always greater than zero when  $s_p(x, t) \neq \Phi$ . However,  $v_g(x, t)$  could be zero due to traffic signals (e.g. queuing traffic as shown in Section 4.1) or stop-and-go traffic condition. In this case,  $v_p(x, t)$  is also zero and there is no relative error in speed for fragment  $x$  at time  $t$ , i.e.  $re_{speed}(x, t) = 0$ .

The overall relative differences at time  $t$  can now be expressed as:

$$re_{density}(t) = \sum_{x:s_p(x,t) \neq \Phi} \frac{l_x(t)}{L_p(t)} \cdot re_{density}(x, t)$$

$$re_{speed}(t) = \sum_{x:s_p(x,t) \neq \Phi} \frac{l_x(t)}{L_p(t)} \cdot re_{speed}(x, t)$$

where  $l_x(t)$  is the length of fragment  $x$  at time  $t$ .

For a simulation of duration  $T$ , define the average of the above performance measures over time as

$$cr_p = \frac{\sum_t cr_p(t)}{T}$$

$$re_{density} = \frac{\sum_t re_{density}(t)}{T}$$

$$re_{speed} = \frac{\sum_t re_{speed}(t)}{T}$$

### 4.1.2 Evaluation Scenarios

In order to analyze the impacts of MPR under different traffic conditions, four scenarios are created. They are low speed low demand (LSLD), low speed high demand (LSHD), high speed low demand (HSLD), and high speed high demand (HSHD). Free flow speeds are 50 km/h and 120 km/h for low- and high-speed settings respectively. The low-demand scenario has a vehicle input of 1,000 vph. This value is increased to 2,000 for the high demand level.

For each traffic scenario, five MPR's, 20%, 50%, 70%, 90% and 100%, are examined. Equipped vehicles are discharged randomly into the simulated traffic flow. More specifically, when a vehicle is generated from the source onto the network, a uniform random number is further generated based on the MPR to determine whether this vehicle is equipped or not. For a given traffic condition scenario and a given MPR, multiple simulation replicates are performed with a range of random seeds of VISSIM traffic simulation. The simulation duration is 180 seconds for each run, with an additional 180-second traffic warm-up period.

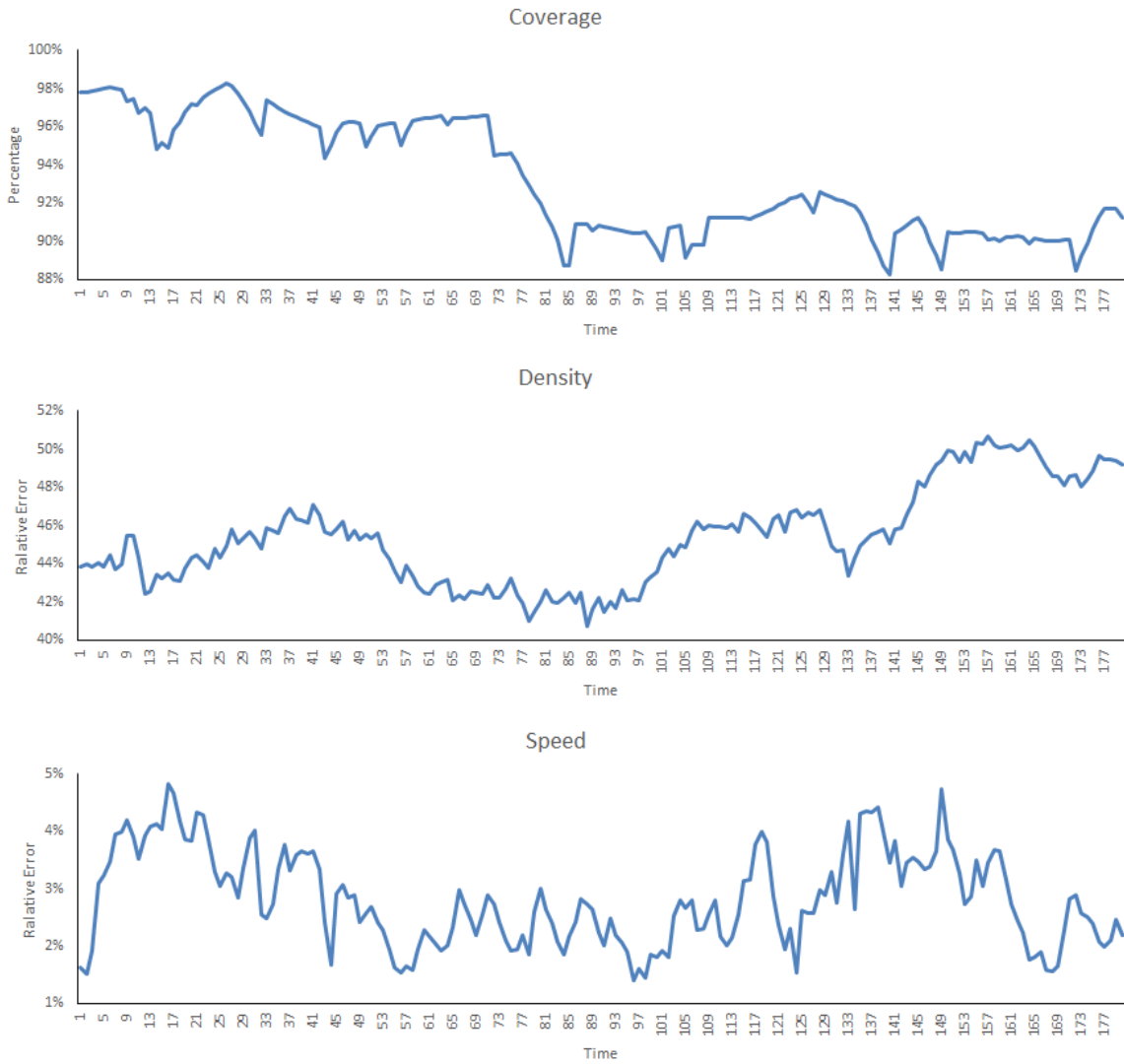
Analysis is performed for both stable and queueing traffic. For the former, a single-lane freeway basic segment of 2365 meters is simulated. For the latter, we used the same freeway segment with the last 1000 meters set as a reduced speed zone in VISSIM. The speed limit for the reduced speed zone is set as 15 km/h for all traffic scenarios.

### 4.1.3 Results Analysis

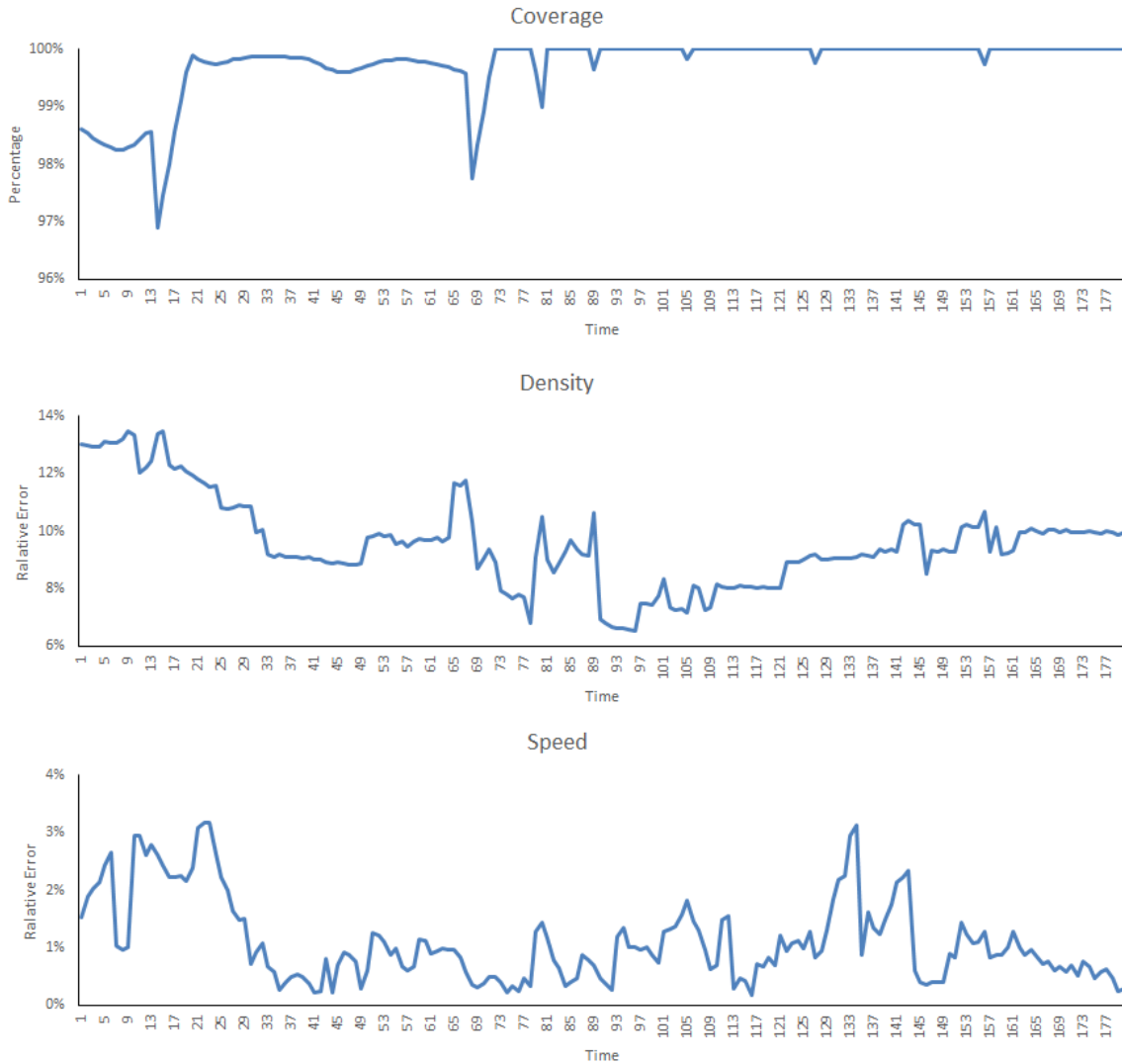
#### 4.1.3.1 *Stable Traffic*

Figure 7 shows the step-by-step outputs of the three performance measures from one representative simulation run with LSHD and 50% MPR. Two phases are observed for the coverage ratio: before and after  $t = 76$ . The coverage ratio is related to the number of equipped vehicles and their spatial distribution. Under this particular scenario, some equipped vehicles have already traversed the road segment at  $t = 76$ . But no new equipped vehicles would enter the roadway as a result of the random number generation. Therefore the coverage ratio is relative high over the first phase, with a sizable decrease after  $t = 76$ . The coverage ratio is always above 88% and the maximum fluctuation is no more than 10% over the entire simulation.  $re_{density}(t)$  is approximately between 40% and 51%. Furthermore, it can be seen from Figure 7 that the relative error in density estimation has increased after  $t = 76$ , suggesting a potential correlation between coverage ratio and  $re_{density}(t)$ .  $re_{speed}(t)$  is rather stable with a maximum of 4.82% and a minimum of 1.40%. No clear trend is observed over time.

Under the same LSHD scenario with the same VISSIM traffic random seed, it can be seen that the coverage ratio towards the end of the simulation is higher and more stable when MPR is increased to 90% (see Figure 8). As expected, the average relative errors of density and speed over time are lower as compared to the 50% MPR scenario.



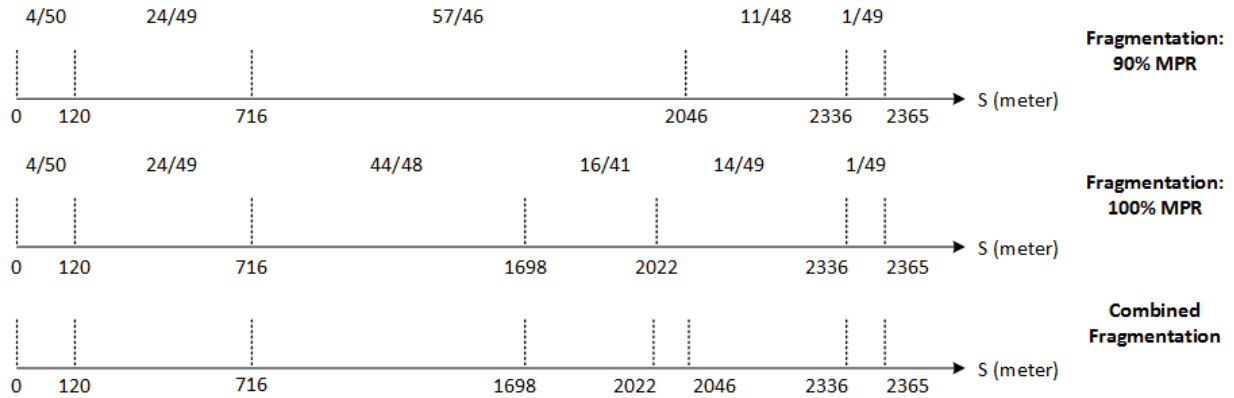
**Figure 7 Step-By-Step Outputs under LSHD Stable Traffic with 50% MPR**



**Figure 8 Step-By-Step Outputs under LSHD Stable Traffic with 90% MPR**

Abrupt changes in relative error of speed are observed at several time steps from Figure 8 (e.g,  $t = 10, 133$ ). To further explain this curious phenomenon, the detailed fragmentation at  $t = 133$  is shown in Figure 9. The pair of numbers above each fragment represents the number of equipped vehicles and the space-mean speed of this fragment. The number below each dashed line indicates the location of a fragment boundary in meters.

Speed differences occur at fragments 716 m – 1,698 m, 1,698 m – 2,022 m, 2,022 m – 2,046 m, and 2,046 m – 2,336 m. The first two fragments are the main cause of the relatively high overall speed relative error of 3.13%. Take the second fragment for example, for the 90% MPR simulation, the space-mean speed is 46 km/h; but it is 41 km/h with 100% MPR, which contributed 1.67% to the overall relative error of 3.13%.



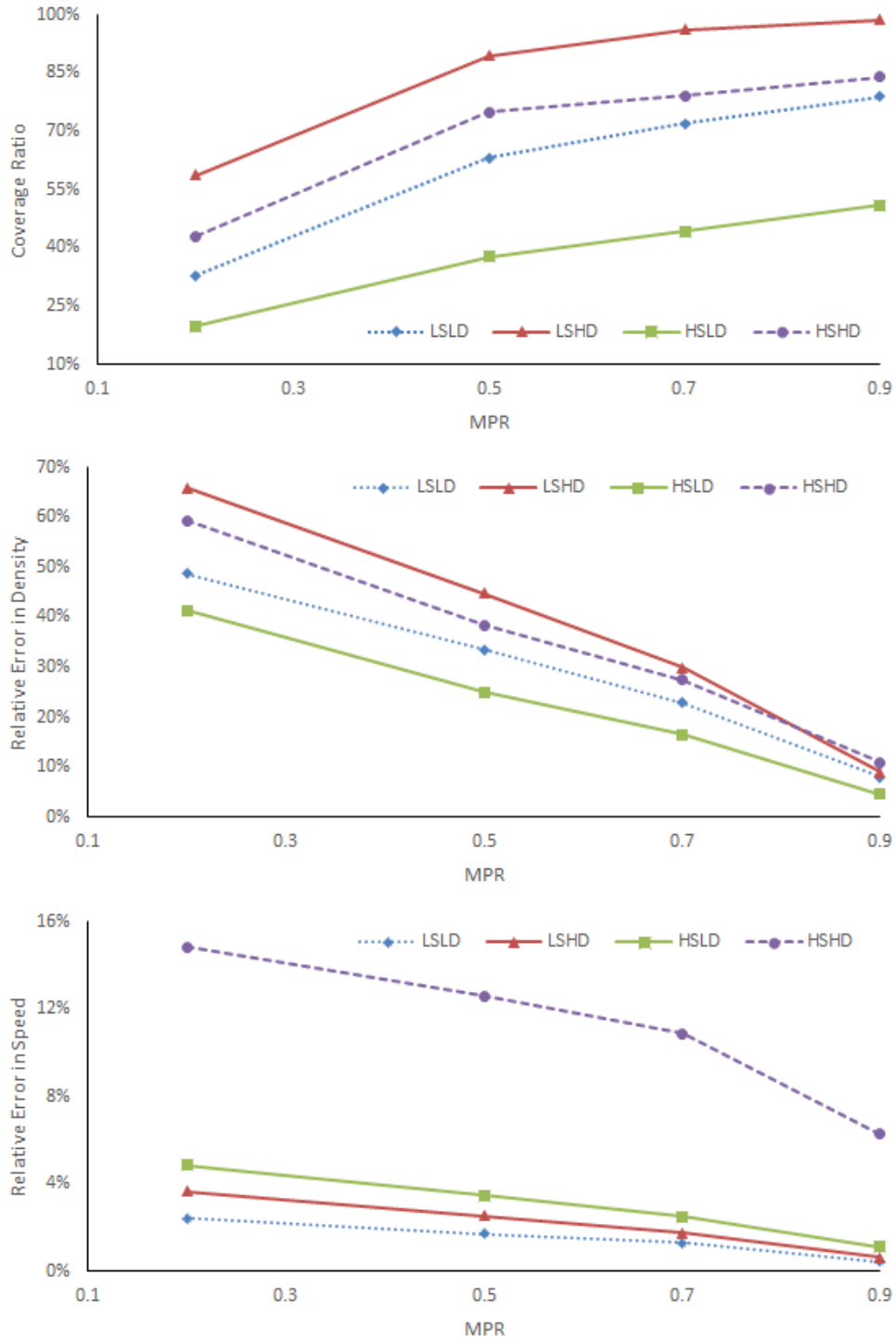
**Figure 9 Detailed Fragmentations at t=133**

Figure 10 shows the three overall performance measures from multiple simulation runs for each traffic scenario and MPR. Nine initial simulation runs are performed for each scenario and each MPR with three traffic random seeds. The mean and standard deviation for each of the three performance measures are then calculated to determine the confidence interval and whether additional runs are needed or not. For five scenarios (HSHD with 50%, 70%, and 90% MPR; LSHD with 20% MPR; LSLD with 20% MPR), it is determined that 20 simulation runs are needed. For the rest of the scenarios, results from the nine initial simulation runs are sufficient to guarantee a 90% confidence interval of  $\pm 0.05$  or tighter. Among those five scenarios requiring additional runs, all but one are able to produce 90% confidence intervals of  $\pm 0.05$  or tighter with 20 simulation runs. Results from the 20 simulation runs for LSHD with 20% MPR have a 90% confidence interval of  $\pm 0.06$ .

It can be observed that the coverage ratio increases with MPR for all four traffic scenarios. When the demand level is fixed, the coverage ratio under low-speed traffic scenarios is always higher than that under high-speed scenarios. This is due to the lower percentage of isolated vehicles under low-speed scenarios. If we fix the speed level, the high-demand scenario results in a higher coverage ratio due to fewer isolated vehicles. In other words, the proposed framework lends itself better to more congested traffic condition for any given MPR, as far as its effectiveness is concerned. Moreover, when  $MPR \geq 50\%$ , the coverage ratio has reached a minimum of 37.76% even under light traffic. This indicates that proposed framework could be useful with an MPR as low as 50%. Even with an MPR of 20%, the coverage ratio, under relatively congested traffic, can still reach around 55.65%.

The average overall relative error in density under each traffic scenario decreases roughly linearly with the increase of MPR. For any MPR (except 90%), LSHD always lead to highest relative error due to the sparsity of vehicles on the road.





**Figure 10 Overall Performance Measures under Stable Traffic**

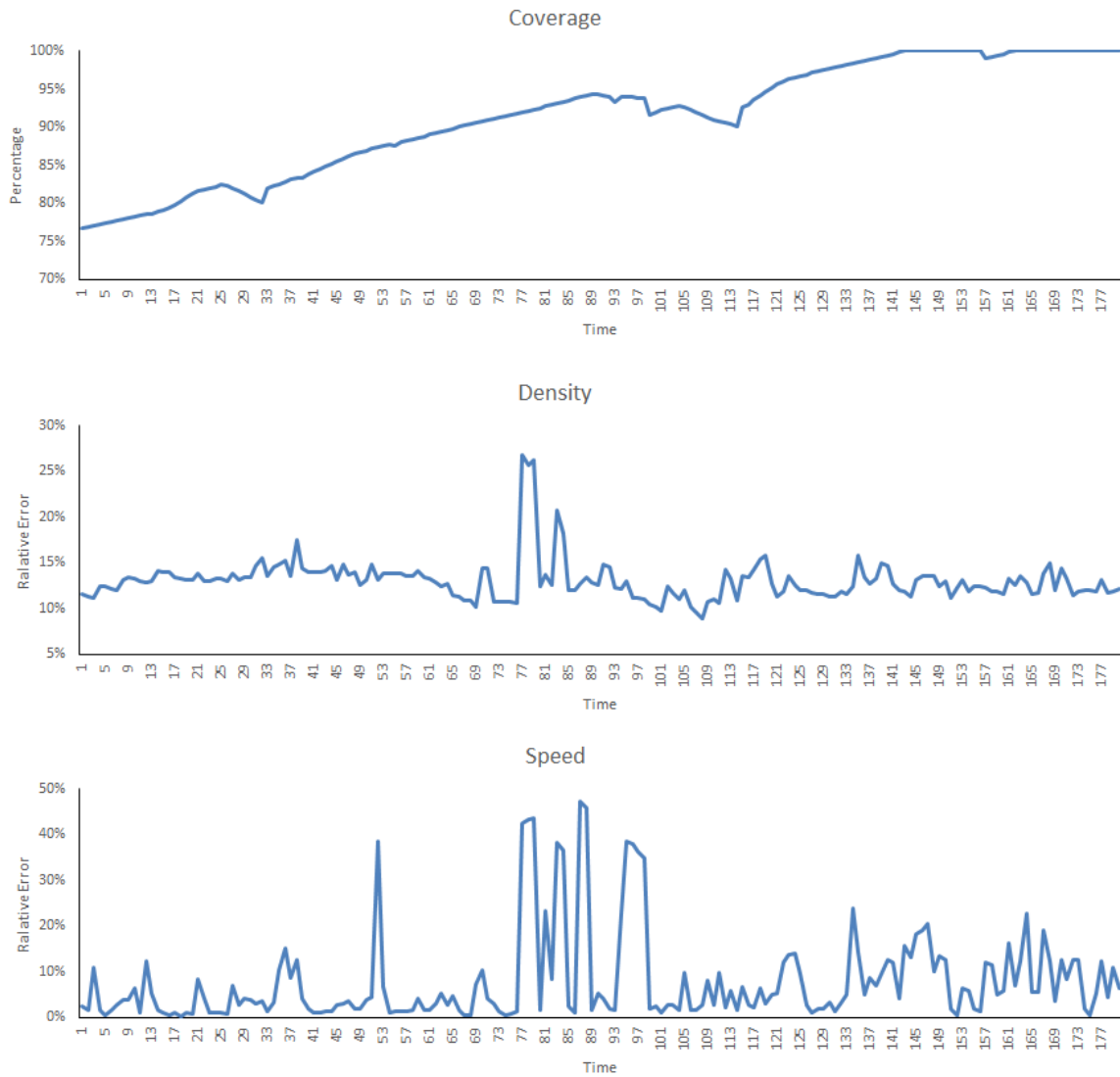
Similarly, the average overall relative error in speed also decreases as MPR increases. It seems that the low-demand scenarios will result in similar relative low errors in speed for any given MPR. For the high-demand scenarios, however, a big difference can be observed between LSHD and HSHD. In fact, it can be seen that the differences among LSLD, and LSHD, HSLD are small, especially with higher MPRs. But HSHD scenario leads to a much higher relative error in

speed. This is because unequipped vehicles do not affect speed estimation very much under relatively stable traffic (in LSLD, LSHD, HSLD scenarios). However, in HSHD scenario, there is a much bigger range of individual vehicle speed distribution, and the impact of MPR is therefore much more pronounced. This also explains that for a given demand level, the scenario with higher speed would observe higher relative error in speed estimation, as seen in Figure 10.

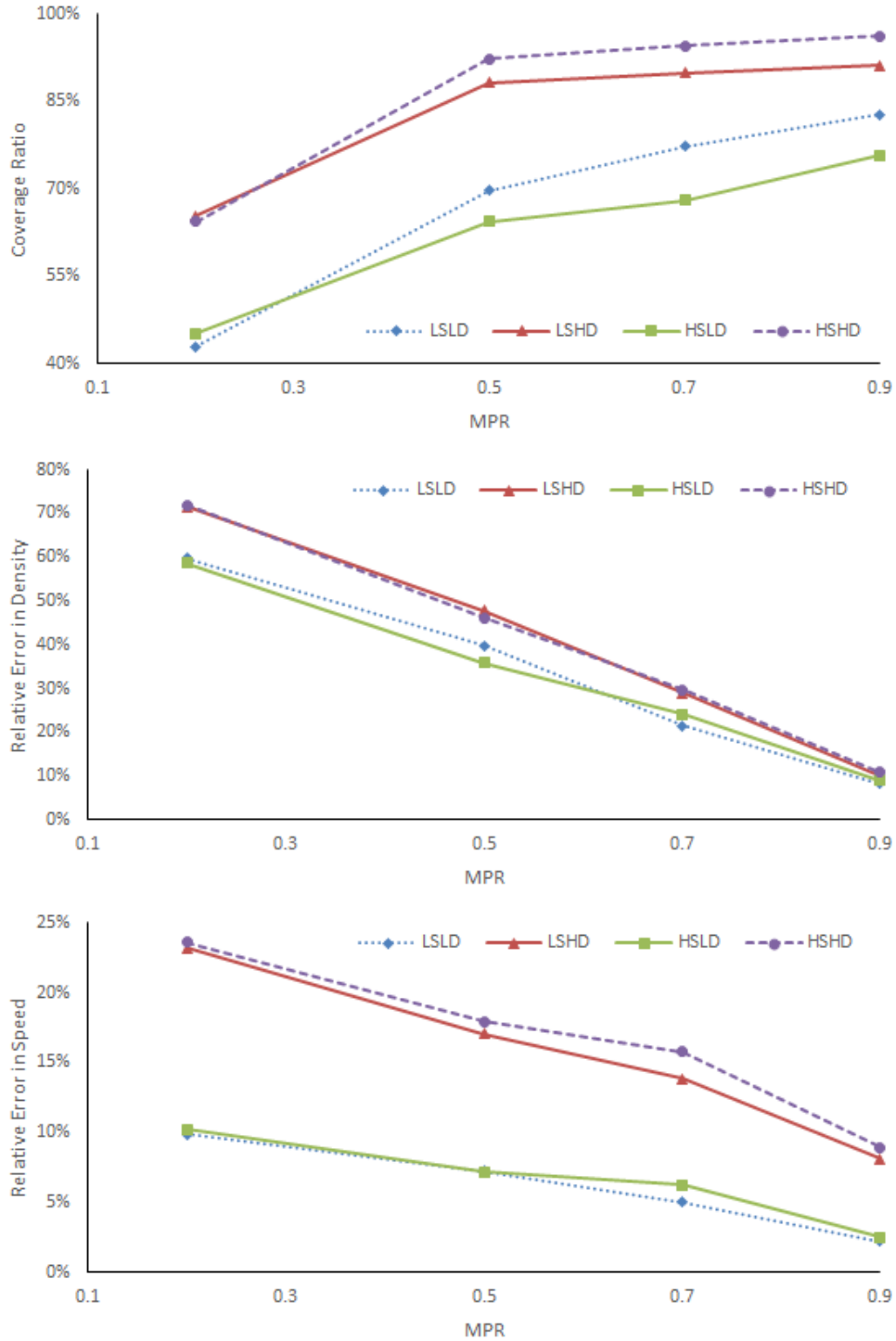
#### 4.1.3.2 *Queueing Traffic*

Figure 11 shows the step-by-step performance of the proposed framework under the LSHD scenario with 90% MPR. As expected, coverage ratio increases with time as vehicles reach the downstream end of the road and more vehicles are on the road. With the introduction of reduced speed zone, it takes longer for vehicles to traverse the road segment compared to the case of stable traffic. In other words, traffic is less evenly distributed on the road at any given time step under queueing traffic comparing to stable traffic. This is why it takes longer for the coverage ratio to reach 90%.

For the other two measures, there is more variation for the relative error in speed compared to that in density. This is directly related to speed fluctuations caused by queueing traffic. As shown in Figure 11, large errors are observed from approximately 77s to 81s for both relative errors. This is because the framework is more sensitive to where equipped vehicles are under queueing traffic as compared to stable traffic, due to the fact that traffic state (speed and density) intrinsically fluctuates more under queueing traffic. Moreover, the platoons detected under queueing traffic tend to be larger than those in stable traffic because of higher congestion. The spatial distribution of unequipped vehicles in this particular simulation run with 90% MPR lead to significantly different fragmentations than those from 100% MPR. For example, at  $t = 77s$ , two major vehicle platoons are identified in case  $g$ , whose locations are 3m – 548m and 595m – 1963m respectively. Under 90% MPR, however, only one major platoon from 3m – 1963m is identified. This is the cause of large errors in both density and speed during 77s to 81s.



**Figure 11 Step-By-Step Outputs under LSHD Queueing Traffic with 90% MPR**



**Figure 12 Overall Performance Measures under Queuing Traffic**

Figure 12 shows that the three performance measures under queuing traffic follow similar trends as stable traffic: coverage ratio increases with MPR, and relative errors in density and speed decrease with MPR. These results are from 9 simulation runs for each scenario and MPR,

except HSLD with 20% MPR, which requires 20 simulation runs. With the respective minimum number of simulation runs, all results have achieved 90% confidence intervals of  $\pm 0.05$  or tighter. Note that the coverage ratio under every traffic scenario with 20% MPR is higher than the corresponding value under stable traffic. This is due to more vehicles on the network caused by queueing. Queueing traffic also leads to more speed fluctuations, which causes the relative error in speed to be more pronounced at low MPRs. These results are as expected.

#### **4.1.3.3                    *Multi-Lane Application***

The distributed traffic monitoring and information aggregation framework can be easily extended from a lane-based system to a link-based system. In this section, we demonstrate its validity and performance by adding one more lane on the roadway network used in previous analyses. All the other settings remain the same. The three performance measures under stable traffic are shown in Figure 13. Compared to stable traffic with single lane, similar trends as are observed (please refer to Section 4.1.3.1 for details). However, the difference between LSLD and HSHD can be ignored for both coverage ratio and relative error in density. For HSHD, the relative error in speed with two lanes is lower than that with single lane.

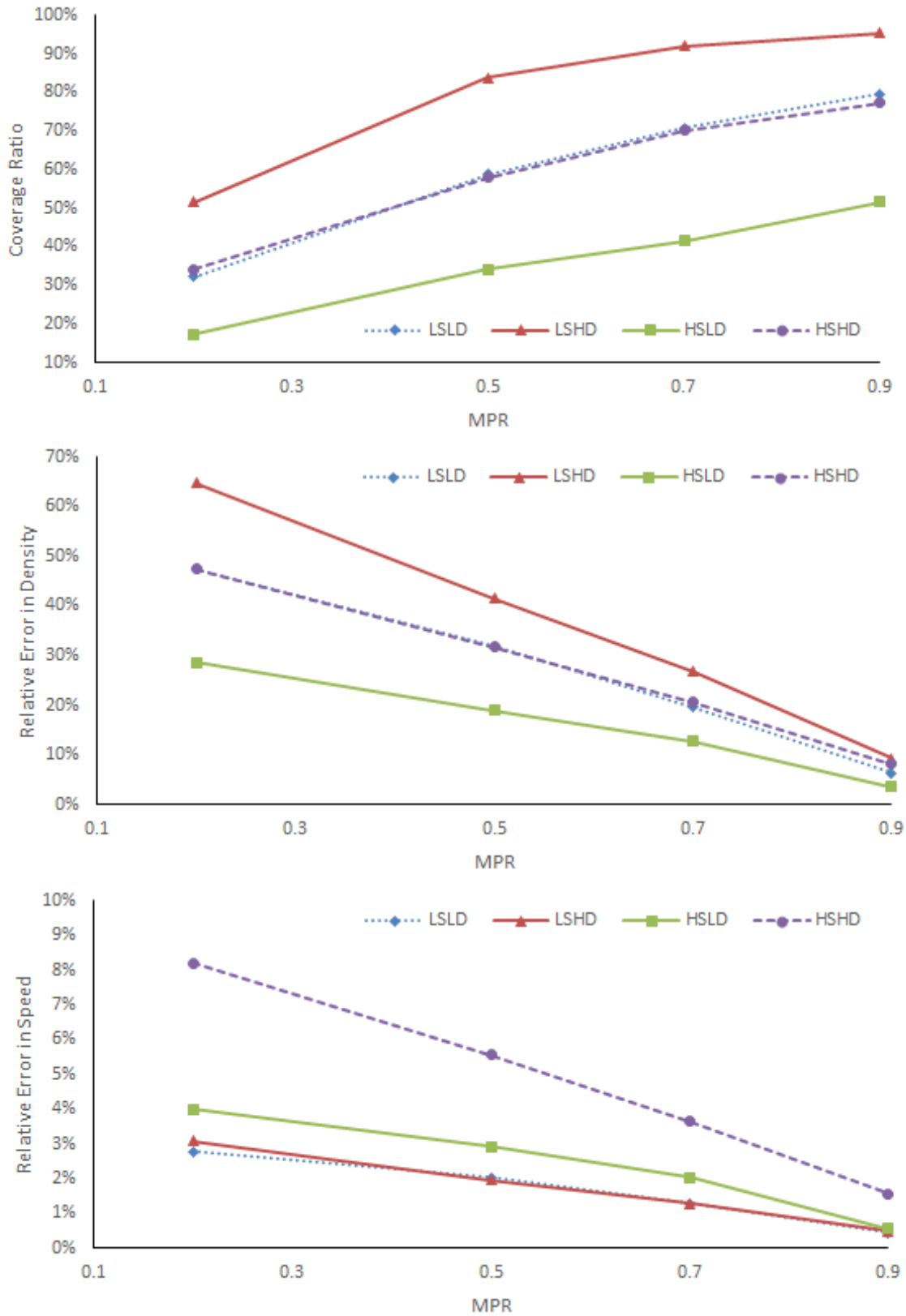
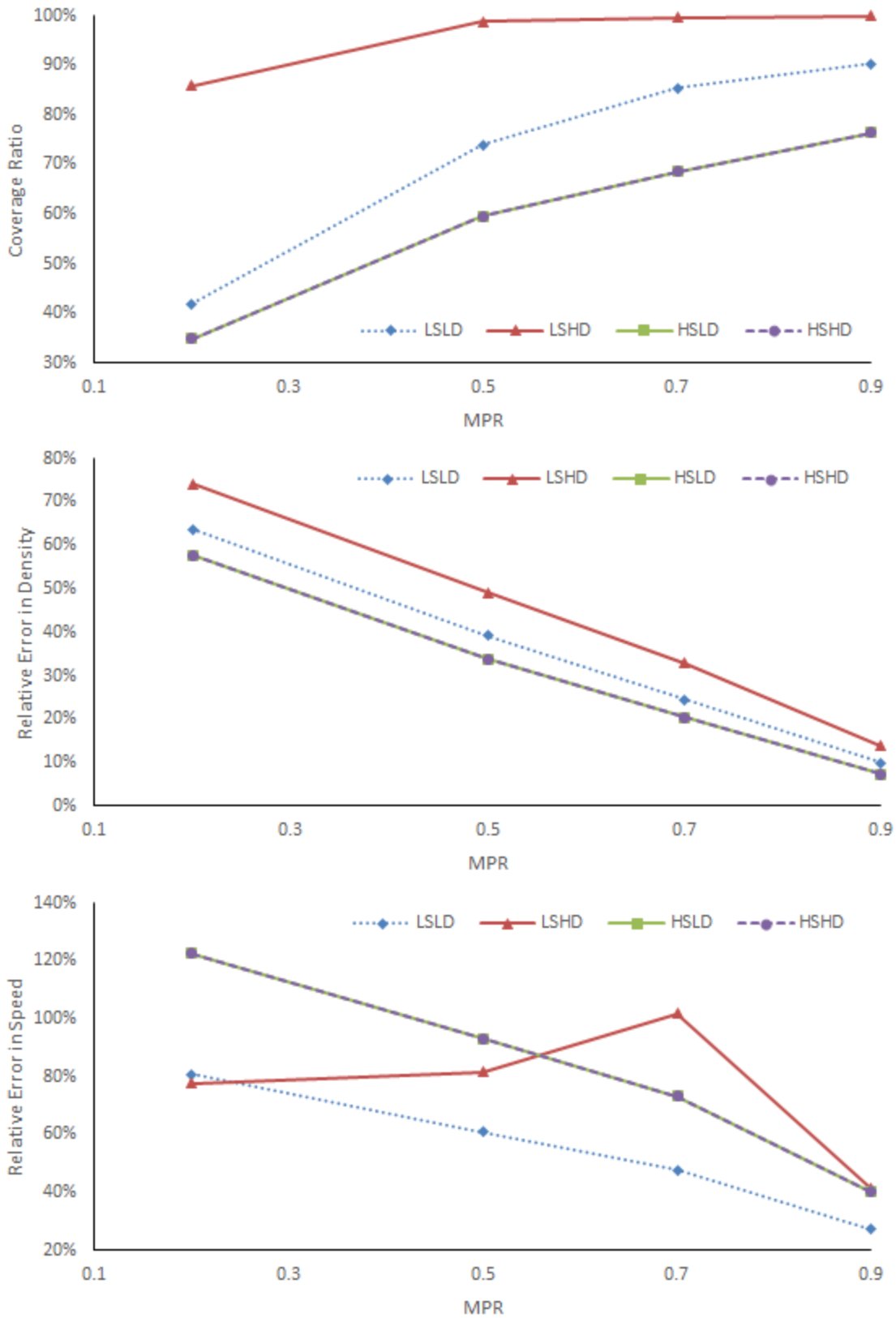


Figure 13 Overall Performance Measures under Stable Traffic with Two Lanes

#### 4.1.3.4 *Interrupted Traffic by Intersection*

In Section 4.1.3.2, we analyzed the performance of the monitoring system under queueing traffic caused by reduced speed zone. Queueing traffic, or more generally, interrupted traffic is highly likely with the presence of intersections, especially signalized intersections. The traffic monitoring and information aggregation framework is able to identify platoons and obtained aggregated traffic information with interrupted traffic with its distributed feature. With the dynamic road fragmentation introduced in Evaluation Methodology, we are able to analyze the system performances under interrupted traffic as the result of intersection. With the presence of a traffic signal controller, spatial and temporal separations are introduced to the traffic flow. Consider a simple traffic network with a single lane, a signal controller placed in the middle of network will divide the network into downstream and upstream segments. Meanwhile, the time domain will be separated into effective green and effective red for each movement. The performance of the monitoring system could be calculated for only the upstream segment, only the downstream segment, or both up- and down-stream segments. Similarly, we could calculate the performance of the monitoring system during the whole cycle, only during effective green, or only during effective red. This leads to  $3 \times 3 = 9$  combinations of time-space windows for our analysis. In this section, we will concentrate on queueing traffic on upstream segment during effective red. The same network as in Section 4.1.3.1 is adopted. A pre-timed traffic signal is placed at 1,000 m downstream from the vehicle input. One different signal timing plan is created with a cycle length of 120s and g/C ratios of 1/3. The overall system performances are illustrated in Figure 14. The coverage ratio, relative error in density, and relative error in speed (except LSHD) under interrupt traffic basically follow the corresponding trends under stable traffic with single lane. For LSHD, the coverage ratio is almost when MPR is greater than or equal to 50%. Traffic signals are going to cause more fluctuations on speed compared to reduced speed zone. The maximal error in speed is over 120%. When  $MPR < 70\%$ , the relative error in speed increases and reaches the maximum at  $MPR=70\%$ .



**Figure 14 Overall Performance Measures under Interrupted Traffic**



## 5.0 PREDICTION ON EVOLUTION OF MICRO-DISCONTINUITY

In Chapter 3, we adopted the concept of micro-discontinuity to measure traffic state difference and thus to identify potential vehicular platoons. A vehicular platoon is uniquely determined by a lead and an anchor vehicle. Isolated vehicles are treated as a special case of micro-discontinuity. Vehicular platoons are directly related to traffic conditions and are subject to change over time especially with queueing traffic. With the distributed traffic monitoring and information aggregation system, we are able to detect the status of micro-discontinuities and track the evolution of platoons at any time. However, it is also important to predict the evolution of platoons for a short time period into the future, which is a key input to designing an effective and efficient virtual transportation operation system.

Figure 15 illustrates the process of platoon evolution. There is only one vehicular platoon at the beginning. With the presence of new anchors and leads from upstream, the platoon evolves into two small platoons at  $t = 71s$ , which represent stopped vehicles and approaching vehicles respectively. But it is not easy to model the evolution. The existing platoon dispersion models cannot track and predict the evolution at such a microscopic level. However, the evolution of platoons is equivalent to that of micro-discontinuities. Therefore, we could predict the evolution of micro-discontinuities instead of making prediction on that of platoons directly. In this section, we propose a framework for predicting evolution of micro-discontinuities near a signalized intersection with given signal timing plans. The framework will perform on the basis of the proposed distributed traffic monitoring and information aggregation system. Two different prediction methodologies will be investigated accordingly.

This section primarily investigates evolution of micro-discontinuities identified by the proposed distributed traffic monitoring system and develop a predication framework. Traffic control information at intersections (for example, signal timing) is considered given in the proposed study. Compared to free flow traffic, queueing traffic will result into more fluctuation into the evolution of micro-discontinuities which is more of interest. This section concentrates on queueing traffic under light and heavy traffic respectively at a signalized intersection.

For light traffic, vehicular platoons are separated by large space headways and the movements of the identified discontinuities are approximately the same as the platoons. As shown in Figure 16, while the lead is always the first vehicle at the stop bar, the evolution of anchor basically follows the trajectory of the last vehicle in the first identified platoon starting from  $t = 265s$ . This can be considered a shockwave prorogated forward incurred by the interactions of the two adjacent platoons which are stopped vehicles and approaching vehicles respectively. With this observation, shockwave analysis from macroscopic traffic flow theories are explored to track the movement of anchors.

For heavy traffic, the evolution of micro-discontinuities are not stationary and back-and-forth movements can be observed over a successive time period. As shown in Figure 17, the anchor of the first vehicular platoon jumped from a downstream position to further upstream at  $t = 282s$

and then moved to further downstream again. The methodology used for light traffic cannot be applied. A localized cooperative mechanism with consideration of individual movements of vehicles within the platoon as inputs that runs on individual vehicles may be needed. The mechanism will be triggered once the value of  $\Delta$  is above a predefined threshold. It should predict whether the platoon will stay together or split into multiple ones in the next several time intervals.

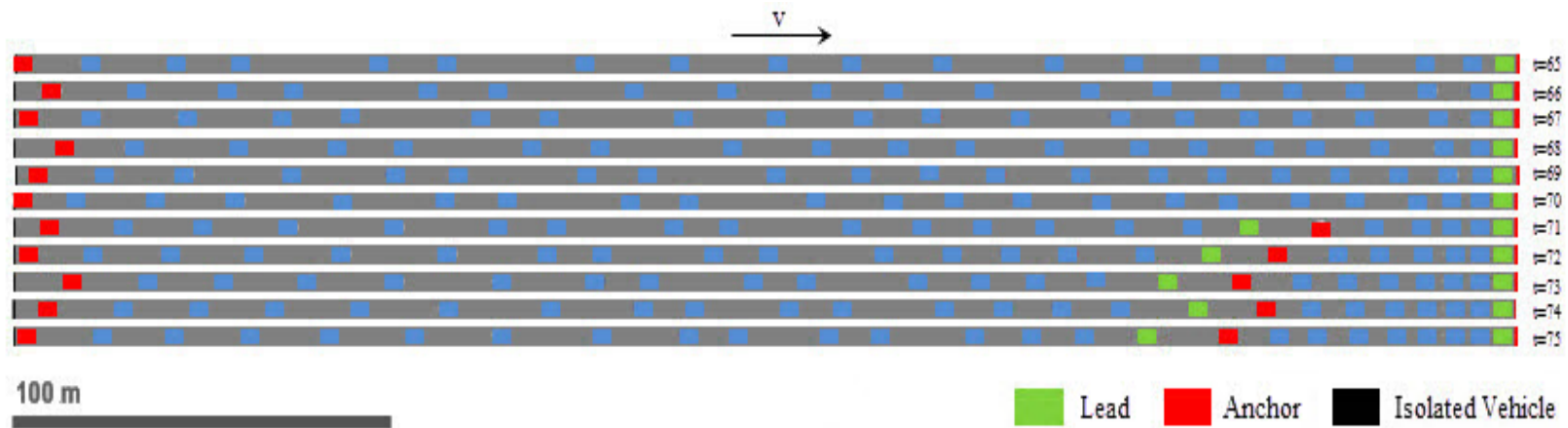


**Figure 15 Evolution of Platoons**

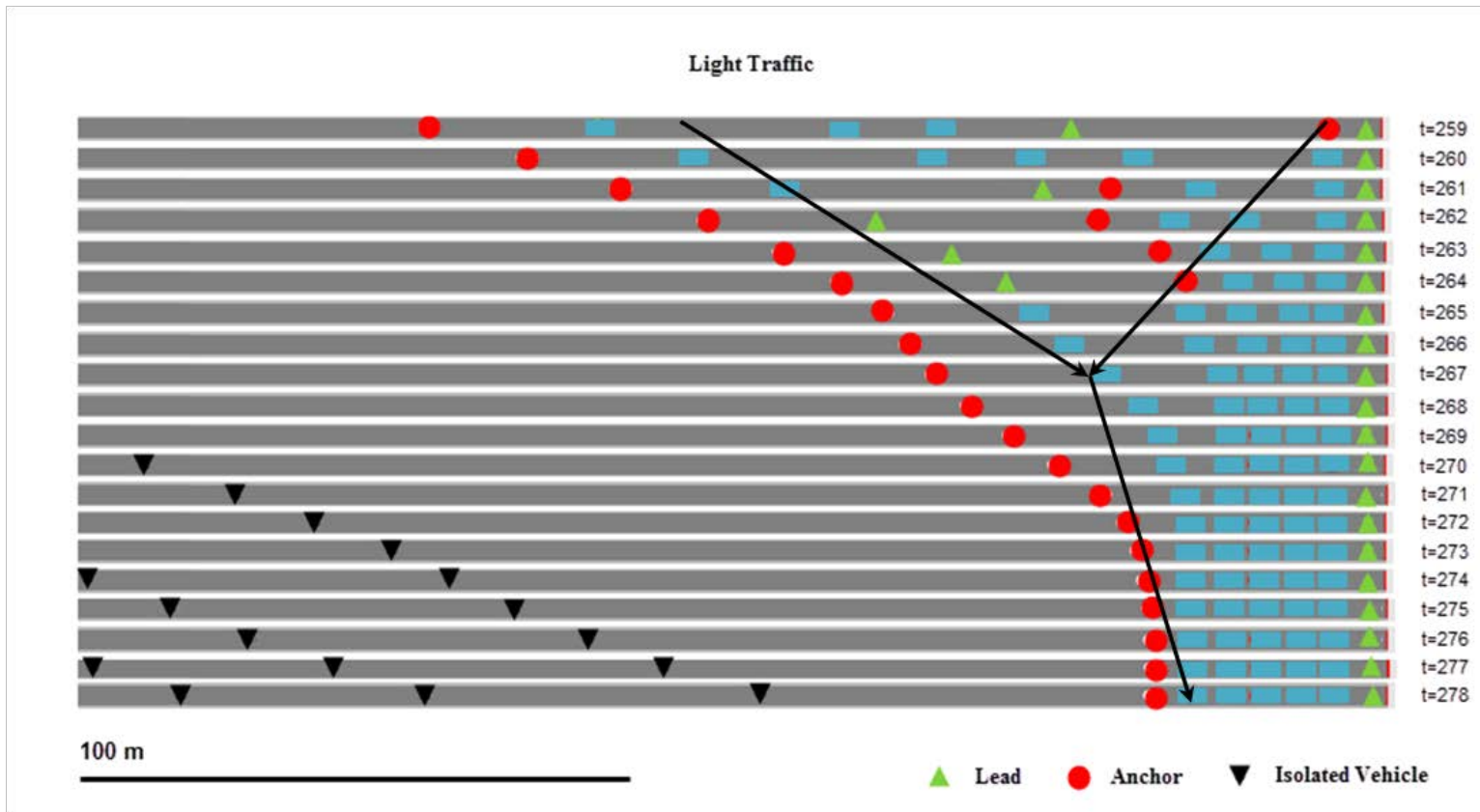


**Figure 16 Evolution of Micro-Discontinuity under Light Traffic**

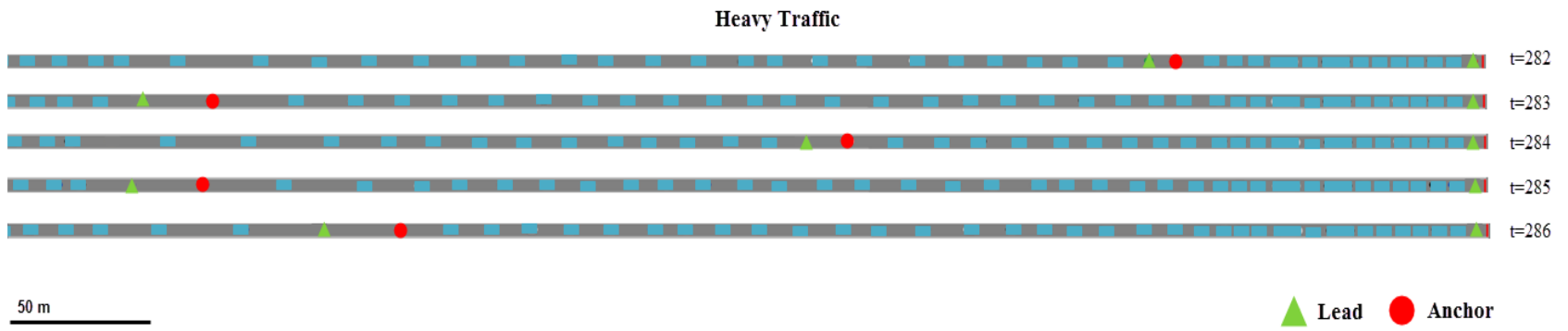


**Figure 17 Evolution of Micro-Discontinuity under Heavy Traffic**

## 6.0 CONCLUSIONS

In this study, we have proposed a distributed framework for network-wide traffic monitoring and platoon information aggregation using V2V DSRC alone. Through distributed protocols, each vehicle will monitor its local traffic condition, flag itself as either the lead or the anchor of a vehicle platoon as appropriate, and validate and self-correct its flag by communicating with its immediate up- and down-stream vehicles. A contention-based cooperative multi-hop information forwarding protocol is developed to make sure that platoon information is aggregated in the most effective and accurate manner with minimum communication overhead. The framework is tested using VISSIM and its built-in COM. A simple freeway and a freeway with a reduced speed zone are created to test the framework under stable traffic and unstable traffic (namely, a queue being formed). The framework is proved to be valid. A new evaluation methodology is proposed to investigate the impact of MPR on the proposed framework. The results suggest that the average coverage ratio increases with MPR. With 50% MPR, the framework is able to provide information coverage for at least 37.76% of the simulated roadway facility. This indicates that the proposed framework could be useful with an MPR as low as 50%. Even with an MPR of 20%, the coverage ratio, under relatively congested traffic, can still reach around 55.65%. The framework is able to provide accurate speed estimation at high spatial resolution for the simulated roadway facility. The maximum relative error is under 10% for relatively congested traffic even with MPR as low as 20%. When there is a wider range of speed distribution (less congested traffic), the worst-case maximum relative error is still under 15% when  $MPR = 20\%$ . The density estimation is more sensitive to MPR, and is more accurate under low demand and high MPR scenarios. As expected, the accuracy of both speed and density estimation increases with MPR for any given traffic scenario. For the simulated roadway facility, we conclude that the proposed framework works better under low-speed high-demand scenarios, and can produce reasonable results with MPR as low as 50%.

As discussed in the manuscript, low MPRs will lead to inferior system performance in terms of all three performance measures. While not much can be done to improve the coverage ratio within the V2V framework, simple adjustments of calculated platoon density can be made to compensate the effect of low MPR. Since platoon density is underestimated with low MPR, one simple adjustment is to divide the original calculated density by the MPR. Simulations with such adjustments were conducted. It is found that this simple adjustment is somewhat effective when MPR is extremely low (20%). For MPRs higher than 50%, the adjustment does not lead to significant performance improvement, and tends to overestimate density. Therefore, we do not recommend this simple adjustment for higher MPRs. Another possible approach is to adjust the calculated density based on macroscopic traffic flow characteristics. However, since the proposed platoon identification and traffic monitoring framework is not on a macroscopic scale, the applicability of traffic stream properties on the identified platoons is questionable. Moreover, this approach would either require pre-loaded traffic stream models into each vehicle or some learning mechanism (which could be both communication and computation intensive) running on each vehicle. Therefore, we recommend at least 50% MPR and no adjustment to keep the proposed framework simple and light.

Although the simulation in this work only focused on a single-lane road section, the proposed framework does not restrict itself to single-lane applications. Under multi-lane scenario, each equipped vehicle will still maintain a set of its surrounding equipped vehicles (including vehicles traveling in the same direction from its own lane and other lanes). The micro-discontinuity identification process and self-correcting mechanism can be easily extended from single lane to multiple lanes, through an additional subroutine to perform a slightly more complicated calculation of relative position along the centerline of the road. After these processes are performed, a link-based platoon will have unique micro-discontinuity flags for its lead and anchor respectively, which would guarantee the proper implementation of the information aggregation process. The application of the proposed framework to multi-lane scenarios is currently being tested and will be presented in our follow-up research paper.

The proposed framework provides fundamental support to an alternative / supplemental traffic operation and management system for transportation networks supported solely by V2V DSRC. The envisioned system is self-sustained, and thus will provide desired redundancy and is particularly suitable for facilitating mobility during the aftermath of extreme events. The envisioned system would also require a methodology for traffic state estimation and prediction as well as algorithms for traffic control and management to improve traffic mobility. These components of the envisioned system will be investigated in our future research.

## 7.0 REFERENCES

- Ban, X. (Jeff), Hao, P., Sun, Z., 2011. Real time queue length estimation for signalized intersections using travel times from mobile sensors. *Transp. Res. Part C Emerg. Technol.* 19, 1133–1156. doi:10.1016/j.trc.2011.01.002
- Bauza, R., Gozalvez, J., Sanchez-Soriano, J., 2010. Road traffic congestion detection through cooperative Vehicle-to-Vehicle communications. *Proc. - Conf. Local Comput. Networks, LCN* 606–612. doi:10.1109/LCN.2010.5735780
- Chaudhary, N. a, Abbas, M.M., Charara, H., Parker, R., 2003. Platoon identification and accommodation system for isolated traffic signals on arterials.
- Christofa, E., Argote, J., Skabardonis, A., 2013. Arterial Queue Spillback Detection and Signal Control Based on Connected Vehicle Technology, in: *The 2013 Annual Meeting Compendium of Papers*. Transportation Research Board, Washington, D.C.
- Comert, G., Cetin, M., 2011. Analytical evaluation of the error in queue length estimation at traffic signals from probe vehicle data. *IEEE Trans. Intell. Transp. Syst.* 12, 563–573. doi:10.1109/TITS.2011.2113375
- Comert, G., Cetin, M., 2009. Queue length estimation from probe vehicle location and the impacts of sample size. *Eur. J. Oper. Res.* 197, 196–202. doi:10.1016/j.ejor.2008.06.024
- Dornbush, S., Joshi, A., 2007. Street Smart Traffic Discovering and Disseminating Automobile Congestion Using VANET's, in: *IEEE 65th Vehicular Technology Conference, 2007*. IEEE, Dublin, pp. 11–15. doi:10.1109/VETECS.2007.15
- Feng, Y., Khoshmagham, S., Zamanipour, M., Head, K.L., 2015. A real-time adaptive signal phase allocation algorithm in a connected vehicle environment, in: *The 2015 Annual Meeting Compendium of Papers*. Transportation Research Board, Washington, D.C.
- Fukumoto, J., Sirokane, N., Ishikawa, Y., Wada, T., Ohtsuki, K., Okada, H., 2007. Analytic method for real-time traffic problems by using Contents Oriented Communications in VANET. *ITST 2007 - 7th Int. Conf. Intell. Transp. Syst. Telecommun. Proc.* 40–45. doi:10.1109/ITST.2007.4295830
- Füßler, H., Widmer, J., Käsemann, M., Mauve, M., Hartenstein, H., 2003. Contention-based forwarding for mobile ad hoc networks. *Ad Hoc Networks* 1, 351–369. doi:10.1016/S1570-8705(03)00038-6
- Goodall, N., Smith, B., Park, B., 2013. Traffic Signal Control with Connected Vehicles. *Transp. Res. Rec. J. Transp. Res. Board* 2381, 65–72. doi:10.3141/2381-08
- Hao, P., Ban, X. (Jeff), 2013. Long Queue Estimation Using Short Vehicle Trajectories for Signalized Intersections, in: *The 2013 Annual Meeting Compendium of Papers*. Transportation Research Board, Washington, D.C.



- He, Q., Head, K.L., Ding, J., 2012. PAMSCOD: Platoon-based arterial multi-modal signal control with online data. *Transp. Res. Part C Emerg. Technol.* 20, 164–184. doi:10.1016/j.trc.2011.05.007
- Huang, D., Shere, S., Ahn, S., 2010. Dynamic highway congestion detection and prediction based on shock waves. *Proc. seventh ACM Int. Work. Veh. InterNETworking - VANET '10* 11–20. doi:10.1145/1860058.1860061
- Jiang, Y., Li, S., Shamo, D.E., 2006. A platoon-based traffic signal timing algorithm for major-minor intersection types. *Transp. Res. Part B Methodol.* 40, 543–562. doi:10.1016/j.trb.2005.07.003
- Jin, W.-L., Recker, W.W., 2006. Instantaneous information propagation in a traffic stream through inter-vehicle communication. *Transp. Res. Part B Methodol.* 40, 230–250. doi:10.1016/j.trb.2005.04.001
- Jin, W.-L., Yang, H., 2013. The Lighthill-Whitham-Richards Model for a Platoon of Vehicles, in: *The 2013 Annual Meeting Compendium of Papers*. Transportation Research Board, Washington, D.C.
- Lakas, A., Cheqfah, M., 2009. Detection and dissipation of road traffic congestion using vehicular communication. *2009 Mediterranean Microw. Symp. MMS 2009*. doi:10.1109/MMS.2009.5409762
- Li, J.-Q., Zhou, K., Shladover Steven, E., Skabardonis, A., 2013. Estimating Queue Length Under Connected Vehicle Technology: Using Probe Vehicle, Loop Detector, and Fused Data, in: *The 2013 Annual Meeting Compendium of Papers*. Transportation Research Board, Washington, D.C.
- Lighthill, M.J., Whitham, G.B., 1955. On Kinematic Waves. II. A Theory of Traffic Flow on Long Crowded Roads. *Proc. R. Soc. A Math. Phys. Eng. Sci.* 229, 317–345. doi:10.1098/rspa.1955.0089
- Lin, L., Osafune, T., 2011. Road congestion detection by distributed vehicle-to vehicle communication systems. US 7,877,196 B2.
- Richards, P.I., 1956. Shock Waves on the Highway. *Oper. Res.* 4, 42–51.
- Stephanopoulos, G., Michalopoulos, P.G., Stephanopoulos, G., 1979. Modelling and analysis of traffic queue dynamics at signalized intersections. *Transp. Res. Part A Gen.* 13, 295–307. doi:10.1016/0191-2607(79)90028-1
- Terroso-sáenz, F., Valdés-vela, M., Sotomayor-martínez, C., Toledo-moreo, R., Gómez-skarmeta, A.F., 2012. Detection With Complex Event Processing and VANET. *IEEE Trans. Intell. Transp. Syst.* 13, 914–929. doi:10.1109/TITS.2012.2186127
- Vaqar, S. a., Basir, O., 2009. Traffic pattern detection in a partially deployed vehicular Ad Hoc network of vehicles. *IEEE Wirel. Commun.* 16, 40–46. doi:10.1109/MWC.2009.5361177